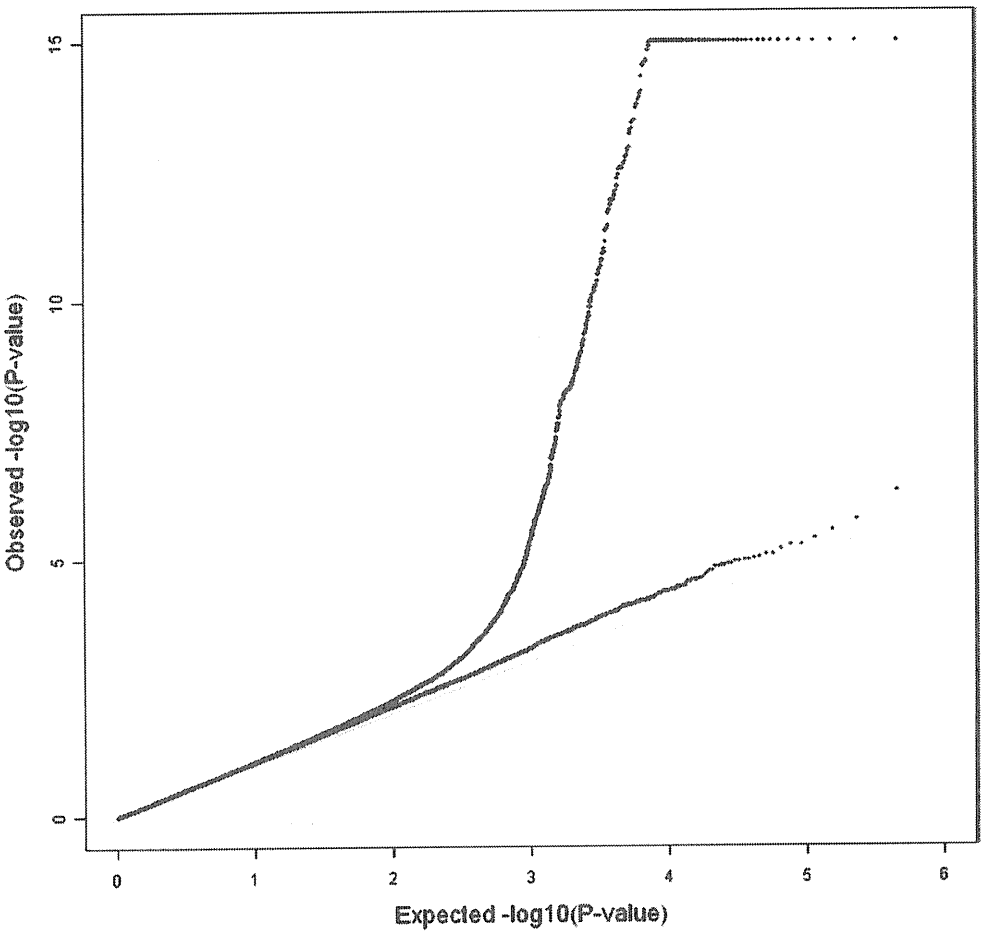

Supplementary Figure 3. Quantile-Quantile plot (QQ-plot) of *P* values in the GWAS. The QQ-plot of Cochran–Armitage trend test *P* values in the GWAS is on a logarithmic scale. The x-axis represents the expected *P* values under the assumption of a uniform distribution of *P* values, and the y-axis represents the observed *P* values in the GWAS. The QQ-plot for the *P* values of all the SNPs that passed the quality control criteria is indicated in *black*. The QQ-plot for the *P* values after the removal of the SNPs included in the MHC region is indicated in *blue*. The SNPs for which the *P* value was $<1.0 \times 10^{-15}$ are indicated at the upper limit of the plot. The *gray dotted line* indicates y = x.

Supplementary Table 1. Associations of HLA-C/B/DRB1/DPB1 Alleles Between UC Cases and CD Cases

	No. of alleles			Allele frequency			UC vs CD		UC vs control[a]		CD vs control[a]	
HLA allele	UC	CD	Control	UC	CD	Control	OR (95% CI)[b]	*P* value[b]	OR (95% CI)[b]	*P* value[b]	OR (95% CI)[b]	*P* value[b]
HLA-C												
Cw*0102	108	151	333	0.15	0.20	0.18	0.66 (0.51–0.87)	.0030				
Cw*0103	3	5	4	0.004	0.007	0.002	0.60 (0.09–3.08)	.51				
Cw*0302	2	7	17	0.003	0.009	0.009	0.28 (0.03–1.49)	.11				
Cw*0303	73	87	191	0.098	0.117	0.106	0.82 (0.59–1.14)	.23				
Cw*0304	77	81	193	0.10	0.11	0.11	0.94 (0.68–1.31)	.72				
Cw*0323	1	0	0	0.001	0	0	—	1				
Cw*0401	21	24	80	0.028	0.032	0.044	0.87 (0.48–1.57)	.64				
Cw*0403	0	0	1	0	0	0.001	—	1				
Cw*0501	1	4	7	0.001	0.005	0.004	0.25 (0.01–2.52)	.22				
Cw*0520	0	1	0	0	0.001	0	0.00 (0.00–38.9)	.50				
Cw*0602	4	8	20	0.005	0.011	0.011	0.50 (0.15–1.65)	.24				
Cw*0701	0	1	2	0	0.001	0.001	0.00 (0.00–38.9)	.50				
Cw*0702	92	83	216	0.12	0.11	0.12	1.12 (0.82–1.54)	.48				
Cw*0704	3	9	14	0.004	0.012	0.008	0.33 (0.09–1.22)	.081				
Cw*0801	36	54	145	0.048	0.073	0.080	0.65 (0.42–1.00)	.049				
Cw*0803	8	9	20	0.011	0.012	0.011	0.89 (0.34–2.31)	.80				
Cw*1202	218	57	251	0.29	0.077	0.14	4.98 (3.64–6.81)	7.4E–27	2.57 (2.09–3.17)	5.5E–20	0.52 (0.38–0.70)	1.3E–05
Cw*1203	2	2	4	0.003	0.003	0.002	1.00 (0.07–13.8)	1				
Cw*1214	0	0	1	0	0	0.001	—	1				
Cw*1402	37	83	134	0.050	0.11	0.074	0.42 (0.28–0.62)	1.1E–05	0.65 (0.45–0.95)	.026	1.58 (1.18–2.10)	.0019
Cw*1403	38	51	115	0.051	0.069	0.064	0.73 (0.47–1.12)	.15				
Cw*1502	20	25	62	0.027	0.034	0.034	0.79 (0.44–1.44)	.44				
HLA-B												
B*0702	31	21	102	0.042	0.028	0.056	1.50 (0.85–2.63)	.16				
B*1301	8	6	15	0.011	0.008	0.008	1.34 (0.46–3.87)	.59				
B*1302	4	2	2	0.005	0.003	0.001	2.00 (0.29–22.2)	.69				
B*1401	0	1	0	0	0.001	0	0.00 (0.00–39.0)	1				
B*1501	42	38	126	0.056	0.051	0.070	1.11 (0.71–1.75)	.65				
B*1507	1	2	19	0.001	0.003	0.011	0.50 (0.01–9.62)	1				
B*1511	3	7	14	0.004	0.009	0.008	0.43 (0.11–1.65)	.20				
B*1518	8	15	25	0.011	0.020	0.014	0.53 (0.22–1.25)	.14				
B*1527	0	1	1	0	0.001	0.001	0.00 (0.00–39.0)	1				
B*2704	3	1	3	0.004	0.001	0.002	3.01 (0.24–158.0)	.62				
B*2705	1	1	1	0.001	0.001	0.001	1.00 (0.01–78.6)	1				
B*3501	51	57	115	0.069	0.077	0.064	0.89 (0.60–1.31)	.55				
B*3701	0	6	17	0	0.008	0.009	0.00 (0.00–0.85)	.031				
B*3801	1	0	2	0.001	0	0.001	—	1				
B*3802	4	2	2	0.005	0.003	0.001	2.00 (0.29–22.2)	.69				
B*3901	26	32	52	0.035	0.043	0.029	0.81 (0.48–1.37)	.42				
B*3902	1	3	1	0.001	0.004	0.001	0.33 (0.01–4.15)	.62				
B*3904	0	3	3	0	0.004	0.002	0.00 (0.00–2.42)	.25				
B*3923	1	2	0	0.001	0.003	0	0.50 (0.01–9.62)	1				
B*4001	40	49	104	0.054	0.066	0.058	0.81 (0.52–1.24)	.33				
B*4002	45	55	113	0.060	0.074	0.063	0.81 (0.54–1.21)	.30				
B*4003	3	3	13	0.004	0.004	0.007	1.00 (0.13–7.49)	1				
B*4006	27	43	109	0.036	0.058	0.060	0.61 (0.38–1.00)	.050				
B*4402	1	4	7	0.001	0.005	0.004	0.25 (0.01–2.53)	.37				
B*4403	38	51	115	0.051	0.069	0.064	0.73 (0.47–1.13)	.16				
B*4601	30	45	86	0.040	0.060	0.048	0.65 (0.41–1.05)	.075				
B*4701	0	0	1	0	0	0.001	—	1				
B*4801	15	11	43	0.020	0.015	0.024	1.37 (0.63–3.01)	.43				
B*5101	47	95	160	0.063	0.128	0.089	0.46 (0.32–0.66)	2.3E–05	0.69 (0.50–0.97)	.033	1.51 (1.15–1.97)	.0028
B*5102	2	4	4	0.003	0.005	0.002	0.50 (0.04–3.49)	.69				
B*5201	218	56	247	0.293	0.075	0.137	5.09 (3.72–6.98)	2.3E–27	2.62 (2.13–3.22)	1.6E–20	0.51 (0.38–0.70)	1.3E–05
B*5401	47	74	159	0.063	0.099	0.088	0.61 (0.42–0.89)	.010				
B*5502	15	13	44	0.020	0.017	0.024	1.16 (0.55–2.45)	.70				
B*5504	1	1	2	0.001	0.001	0.001	1.00 (0.01–78.6)	1				
B*5601	4	3	21	0.005	0.004	0.012	1.33 (0.22–9.14)	1				
B*5603	0	3	5	0	0.004	0.003	0.00 (0.00–2.42)	.25				
B*5801	2	7	17	0.003	0.009	0.009	0.28 (0.03–1.50)	.18				
B*5901	10	21	37	0.013	0.028	0.020	0.47 (0.22–1.00)	.046				
B*6701	14	6	19	0.019	0.008	0.011	2.36 (0.90–6.17)	.072				
HLA-DRB1												
DRB1*0101	32	15	105	0.043	0.020	0.058	2.17 (1.16–4.04)	.013				
DRB1*0301	1	3	8	0.001	0.004	0.004	0.33 (0.01–4.12)	.37				
DRB1*0401	4	12	18	0.005	0.016	0.010	0.33 (0.10–1.02)	.043				
DRB1*0403	11	7	62	0.015	0.010	0.034	1.57 (0.60–4.06)	.35				
DRB1*0404	2	2	7	0.003	0.003	0.004	0.99 (0.07–13.7)	1				
DRB1*0405	77	154	234	0.104	0.209	0.129	0.44 (0.33–0.59)	2.4E–08	0.78 (0.59–1.02)	.072	1.78 (1.42–2.23)	3.8E–07
DRB1*0406	17	25	54	0.023	0.034	0.030	0.67 (0.36–1.25)	.20				
DRB1*0407	0	0	5	0	0	0.003	—	1				
DRB1*0410	10	29	24	0.013	0.039	0.013	0.33 (0.16–0.69)	.0019				
DRB1*0701	2	3	5	0.003	0.004	0.003	0.66 (0.06–5.78)	.69				
DRB1*0801	0	0	1	0	0	0.001	—	1				
DRB1*0802	29	51	64	0.039	0.069	0.035	0.55 (0.34–0.87)	.010				
DRB1*0803	63	67	163	0.085	0.091	0.090	0.93 (0.65–1.33)	.68				
DRB1*0901	74	98	283	0.100	0.133	0.157	0.72 (0.52–0.99)	.045				
DRB1*1001	0	5	18	0	0.007	0.010	0.00 (0.00–1.08)	.030				

Supplementary Table 1. (Continued)

	No. of alleles			Allele frequency			UC vs CD		UC vs control[a]		CD vs control[a]	
HLA allele	UC	CD	Control	UC	CD	Control	OR (95% CI)[b]	*P* value[b]	OR (95% CI)[b]	*P* value[b]	OR (95% CI)[b]	*P* value[b]
DRB1*1101	18	19	41	0.024	0.026	0.023	0.94 (0.49–1.80)	.85				
DRB1*1108	0	0	1	0	0	0.001	.....	1				
DRB1*1119	0	1	0	0	0.001	0	0.00 (0.00–38.7)	.50				
DRB1*1123	0	0	1	0	0	0.001	—	1				
DRB1*1201	18	30	71	0.024	0.041	0.039	0.59 (0.32–1.06)	.074				
DRB1*1202	10	7	26	0.013	0.010	0.014	1.42 (0.54–3.76)	.47				
DRB1*1301	2	7	14	0.003	0.010	0.008	0.28 (0.03–1.49)	.11				
DRB1*1302	37	41	97	0.050	0.056	0.054	0.89 (0.56–1.40)	.62				
DRB1*1401	18	37	47	0.024	0.050	0.026	0.47 (0.26–0.83)	.0082				
DRB1*1403	7	12	20	0.009	0.016	0.011	0.57 (0.22–1.47)	.24				
DRB1*1405	15	22	30	0.020	0.030	0.017	0.67 (0.34–1.30)	.23				
DRB1*1406	10	8	21	0.013	0.011	0.012	1.24 (0.49–3.17)	.65				
DRB1*1407	2	2	1	0.003	0.003	0.001	0.99 (0.07–13.7)	1				
DRB1*1429	1	0	1	0.001	0	0.001	—	1				
DRB1*1501	69	32	126	0.093	0.043	0.070	2.26 (1.46–3.48)	1.6E−04	1.37 (1.01–1.86)	.044	0.61 (0.41–0.90)	.013
DRB1*1502	207	44	246	0.279	0.060	0.136	6.09 (4.31–8.59)	3.2E−29	2.46 (1.99–3.03)	9.8E−18	0.40 (0.29–0.56)	4.0E−08
DRB1*1602	6	3	14	0.008	0.004	0.008	1.99 (0.42–12.4)	.51				
HLA–DPB1												
DPB1*0201	114	165	412	0.153	0.222	0.228	0.63 (0.49–0.82)	6.4E−04				
DPB1*0202	28	24	76	0.038	0.032	0.042	1.17 (0.67–2.04)	.58				
DPB1*0301	25	44	62	0.034	0.059	0.034	0.55 (0.33–0.91)	.019				
DPB1*0401	30	30	84	0.040	0.040	0.046	1.00 (0.59–1.67)	.99				
DPB1*0402	53	51	170	0.071	0.069	0.094	1.04 (0.70–1.55)	.85				
DPB1*0501	279	345	698	0.375	0.465	0.386	0.69 (0.56–0.85)	4.4E−04	0.95 (0.80–1.14)	.60	1.38 (1.16–1.64)	.00023
DPB1*0601	5	3	7	0.007	0.004	0.004	1.67 (0.32–10.8)	.73				
DPB1*0901	181	42	226	0.243	0.057	0.125	5.36 (3.76–7.63)	7.1E−24	2.25 (1.81–2.80)	1.2E−13	0.42 (0.30–0.59)	3.1E−07
DPB1*1301	10	14	29	0.013	0.019	0.016	0.71 (0.31–1.61)	.41				
DPB1*1401	11	15	23	0.015	0.020	0.013	0.73 (0.33–1.59)	.42				
DPB1*1701	2	1	2	0.003	0.001	0.001	2.00 (0.10–117.9)	1				
DPB1*1901	6	4	5	0.008	0.005	0.003	1.50 (0.35–7.26)	.75				
DPB1*2501	0	1	0	0	0.001	0	0.00 (0.00–38.9)	.50				
DPB1*3601	0	0	4	0	0	0.002	—	1				
DPB1*3801	0	3	2	0	0.004	0.001	0.00 (0.00–2.41)	.12				
DPB1*4101	0	0	6	0	0	0.003	—	1				
DPB1*4701	0	0	2	0	0	0.001	—	1				

[a]Calculated for the HLA alleles that indicated significant associations between UC cases and CD cases. Based on Bonferroni correction for the number the observed alleles (n = 110), $P < .00045$ was considered to be significant ($\alpha = .05$).
[b]Obtained by the comparison of allele frequencies.

Supplementary Table 2. Case-Case and Case-Control Associations of HLA-Cw*1202-B*5201-DRB1*1502 Haplotype Stratified by Colonic and Noncolonic CD

	Analyzed groups	No. subjects (group 1/group 2)	Frequency (group 1/group 2)	OR (95% CI)	*P* value
Within case analysis	UC vs CD	372/372	0.27/0.054	6.58 (4.60–9.42)	1.1×10^{-33}
	UC vs colonic CD	372/53	0.27/0.10	3.19 (1.67–6.09)	6.4×10^{-5}
	UC vs noncolonic CD	372/315	0.27/0.043	8.36 (5.50–12.72)	8.8×10^{-36}
	Colonic CD vs noncolonic CD	53/315	0.10/0.043	2.62 (1.26–5.48)	.0083
Case-control analysis	UC vs control	372/905	0.27/0.12	2.65 (2.14–3.29)	4.0×10^{-21}
	CD vs control	372/905	0.054/0.12	0.40 (0.28–0.57)	1.1×10^{-7}
	Colonic CD vs control	53/905	0.10/0.12	0.83 (0.44–1.58)	.58
	Noncolonic CD vs control	315/905	0.043/0.12	0.32 (0.21–0.48)	5.2×10^{-9}

SR-PSOX/CXCL16 plays a critical role in the progression of colonic inflammation

Norimitsu Uza,[1] Hiroshi Nakase,[1] Shuji Yamamoto,[1] Takuya Yoshino,[1] Yasuhiro Takeda,[1] Satoru Ueno,[1] Satoko Inoue,[1] Sakae Mikami,[1] Minoru Matsuura,[1] Takeshi Shimaoka,[2] Noriaki Kume,[3] Manabu Minami,[3] Shin Yonehara,[4] Hiroki Ikeuchi,[5] Tsutomu Chiba[1]

► An additional figure is published online only. To view this file please visit the journal online (http://gut.bmj.com).

[1]Department of Gastroenterology and Hepatology, Graduate School of Medicine, Kyoto University, Kyoto, Japan
[2]Department of Molecular Preventive Medicine, Graduate School of Medicine, University of Tokyo, Tokyo, Japan
[3]Department of Cardiovascular Medicine, Graduate School of Medicine, Kyoto University, Kyoto, Japan
[4]Department of Animal Development and Physiology, Graduate School of Biostudies, Kyoto University, Kyoto, Japan
[5]Department of Surgery, Hyogo College of Medicine, Hyogo, Japan

Correspondence to
Professor Hiroshi Nakase, Department of Gastroenterology and Hepatology, Graduate School of Medicine, Kyoto University, 54 Shogoin-Kawara-cho, Sakyo-ku, Kyoto 606-8507, Japan; hiropy@kuhp.kyoto-u.ac.jp

Revised 31 January 2011
Accepted 12 February 2011
Published Online First 6 April 2011

ABSTRACT

Background and aims Inflammatory bowel disease (IBD) is initiated and perpetuated by a dysregulated immune response to unknown environmental antigens such as luminal bacteria in genetically susceptible hosts. SR-PSOX/CXCL16, a scavenger receptor that binds phosphatidylserine and oxidised lipoprotein, has both phagocytic activity and chemotactic properties. The aim of this study was to investigate the role of SR-PSOX/CXCL16 in patients with IBD and experimental murine colitis.

Methods The serum levels of SR-PSOX/CXCL16 were measured in patients with IBD. The roles of SR-PSOX/CXCL16 in phagocytosis of bacterial components and cytokine production by macrophages from wild-type (WT) and SR-PSOX/CXCL16 knockout (KO) mice were assessed. Colitis was induced by administering dextran sulfate sodium (DSS) to WT and SR-PSOX/CXCL16 KO mice. Colonic inflammation was analysed by clinical, histological and immunological parameters. Finally, the effect of a monoclonal antibody (mAb) to SR-PSOX/CXCL16 on DSS-induced colitis and trinitrobenzene sulfonic acid-induced colitis models was evaluated.

Results Serum levels of SR-PSOX/CXCL16 correlated significantly with the disease activity of patients with IBD. Ex vivo experiments showed that SR-PSOX/CXCL16 was involved in both phagocytosis of bacterial antigens and the T helper 1 immune response through the production of interleukin 12 and interferon γ. In vivo murine experiments demonstrated the upregulated gene expression of SR-PSOX/CXCL16 in inflamed colonic tissues and the predominant expression of SR-PSOX/CXCL16 on macrophages. SR-PSOX/CXCL16 KO mice were less susceptible to colonic inflammation than were their WT littermates. Administration of SR-PSOX/CXCL16 mAb ameliorated the condition in the two different experimental colitis models.

Conclusions SR-PSOX/CXCL16 plays a critical role in colonic inflammation and could be a potential therapeutic target for patients with IBD.

Significance of this study

What is already known about this subject?
- Inflammatory bowel disease (IBD) is associated with a dysregulated immune response to unknown environmental antigens including luminal bacteria in genetically susceptible hosts.
- SR-PSOX/CXCL16 is associated with several inflammatory diseases.
- SR-PSOX/CXCL16 is constitutively expressed in the small intestine but not in normal colonic tissues.
- SR-PSOX/CXCL16 has two different biological activities: as a scavenger receptor and as a chemokine.

What are the new findings?
- Serum levels of SR-PSOX/CXCL16 correlated with the disease activity of IBD.
- SR-PSOX/CXCL16 expression is upregulated in inflamed colonic tissues and predominantly detected on macrophages.
- SR-PSOX/CXCL16 is involved in not only phagocytosis of bacterial antigens but also the T helper 1 immune response in the progression of colitis.
- SR-PSOX/CXCL16 monoclonal antibody ameliorated the condition in two different experimental colitis models.

How might it impact on clinical practice in the foreseeable future?
- Our data provide the first evidence for a critical role for SR-PSOX/CXCL16 in the progression of colonic inflammation ex vivo and in vivo. These data suggest that SR-PSOX/CXCL16 could be a potential therapeutic target for patients with IBD.

INTRODUCTION

Inflammatory bowel diseases (IBDs), including Crohn's disease (CD) and ulcerative colitis (UC), are chronic and relapsing-remitting conditions with unknown aetiology. Previous clinical and basic observations suggest that inflammation is initiated and perpetuated by a dysregulated immune response to unknown environmental antigens such as luminal bacteria in genetically susceptible hosts.[1] Recent genome-wide association studies showed that genes involved in both innate and adaptive immune responses could be risk factors for developing IBD.[2 3] Moreover, an abnormal response of intestinal macrophages to commensal bacteria was reported to result in chronic intestinal inflammation.[4] Therefore, it is important to investigate the relationship between luminal bacteria and antigen-presenting cells (APCs) in the pathogenesis of IBD. Indeed, we showed that macrophage-targeting treatment ameliorates colonic inflammation in an experimental colitis model.[5] Thus, the control of

Gut 2011;**60**:1494–1505. doi:10.1136/gut.2010.221879

molecules related to macrophages appears to be a promising approach for the treatment of IBD.

Chemokines are a superfamily of small chemotactic cytokines and are classified into four major subfamilies on the basis of the motif of the first two cysteine residues: CC, CXC, C and CX3C subfamilies.[6] The most important function of chemokines is the ability to regulate leucocyte trafficking and retention in lymphoid tissues and in peripheral tissues in both homeostasis and inflammation.[7 8] The expression of several chemokines increases in the colonic tissues of both experimental murine colitis models and patients with IBD,[9 10] and these chemokines are suggested to play a role in the pathophysiology of colitis.

SR-PSOX/CXCL16, a scavenger receptor that binds phosphatidylserine and oxidised lipoprotein, is a chemokine of the CXC family and has been identified as a novel transmembrane protein.[11–13] In the static state, SR-PSOX/CXCL16 is expressed in various lymphoid tissues including the thymus, spleen, lymph nodes and Peyer's patches, and in non-lymphoid tissues including the lung, liver, kidney and small intestine, but not colonic tissue.[11 12] Among immune cells, SR-PSOX/CXCL16 is found primarily on the surface of APCs such as monocytes/macrophages and dendritic cells.[11–13] SR-PSOX/CXCL16 has two different biological activities: as a scavenger receptor that mediates adhesion and phagocytosis of both Gram-positive and Gram-negative bacteria by APCs[14] and as a chemokine for CXCR6-expressing cells such as naïve CD8 T cells, T helper 1 (Th1)-polarised CD4 and CD8 T cells, and natural killer T cells. Accordingly, it is possible that SR-PSOX/CXCL16 plays an important role in both innate and adaptive immunity by mediating the uptake of bacteria as well as the recruitment of CXCR6-expressing T cells by APCs. Although SR-PSOX/CXCL16 has been shown to be involved in several inflammatory conditions,[15–17] little is known about the function of SR-PSOX/CXCL16 in intestinal inflammation.

The aim of this study was to elucidate the role of SR-PSOX/CXCL16 in the pathophysiology of IBD. We first measured the serum levels of SR-PSOX/CXCL16 in patients with IBD. We assessed the role of SR-PSOX/CXCL16 in phagocytosis of bacterial components and cytokine production by macrophages in SR-PSOX/CXCL16 knockout (KO) mice. Next, we investigated the role of SR-PSOX/CXCL16 in a dextran sulfate sodium (DSS)-induced colitis model. Finally, we examined the effects of a monoclonal antibody (mAb) to SR-PSOX/CXCL16 in two experimental murine colitis models: DSS-induced colitis and 2,4,6-trinitrobenzene sulfonic acid (TNBS)-induced colitis.

MATERIALS AND METHODS

Human serum samples

Human serum samples were obtained from 14 patients (11 men and 3 women; mean age, 27.8±6.4 years) with active CD, 16 patients (9 men and 7 women; 27.7±7.4 years) with inactive CD, 16 patients (10 men and 6 women; 27.2±15.6 years) with active UC, 13 patients (10 men and 3 women; 29.5±14.8 years) with inactive UC and 16 healthy volunteers (15 men and 1 woman; 34.6±3.1 years). The clinical characteristics of patients with CD and UC are shown in table 1. The disease activity of the patients with CD and UC was determined according to the Crohn's Disease Activity Index (CDAI)[18] and the Clinical Activity Index (CAI),[19] respectively. A CDAI ≥150 and a CAI ≥5 was defined as active CD and active UC, respectively.[20 21] Informed consent was obtained from all patients and volunteers, and the experimental design using these samples was approved by the Kyoto University Hospital Ethics Committee.

Table 1 Clinical characteristics of patients

(A) Patients with CD	Active CD (n=14)	Inactive CD (n=16)
Age (years)	27.8±6.4	27.7±7.4
Gender (M/F)	11/3	9/7
Disease duration (years)	8.0±7.3	8.3±7.3
Disease location (n)	Ileal only (3)	Ileal only (8)
	Ileocolonic (7)	Ileocolonic (4)
	Colonic only (4)	Colonic only (4)
CDAI	248.0±87	110.1±25.8*
(B) Patients with UC	**Active UC (n=16)**	**Inactive UC (n=13)**
Age (years)	27.2±15.6	29.5±14.8
Gender (M/F)	10/6	10/3
Disease duration (years)	2.1±1.8	9.1±4.8*
Disease location (n)	Pancolitis (9)	Pancolitis (7)
	Left-sided colitis (7)	Left-sided colitis (5)
	Proctitis (0)	Proctitis (1)
CAI	10.9±2.9	1.2±1.2*

The values are expressed as mean±SD or number of patients.
*$p<0.01$ between active and inactive CD or UC.
CAI, Clinical Activity Index; CD, Crohn's disease; CDAI, Crohn's Disease Activity Index; F, female; M, male, UC, ulcerative colitis.

Mice

SR-PSOX/CXCL16 KO mice were generated in collaboration with Sankyo Co. (Tokyo, Japan) as described previously.[22] Heterozygous mice were generated by crossing SR-PSOX/CXCL16 KO mice and C57BL/6 mice, and were intercrossed to obtain homozygous SR-PSOX/CXCL16 KO and wild-type (WT) littermates. The genotyping of F_2 mice was performed by PCR at least twice using the following primers: 5′-TACCGCAGGGTACTTTGGATCA-3′ and 5′-TTGCGCTCAAAGCAGTCCACTA-3′ for detection of the WT SR-PSOX/CXCL16 allele (351 bp), and 5′-GGATCTCCTGTCATCTCACCTTGC-3′ and 5′-CGGCCACAGTCGATGAATCCAGAA-3′ for detection of the KO allele (333 bp). SR-PSOX/CXCL16 KO mice and their WT littermates from intercrosses of heterozygous mice were used in the experiments. C57BL/6 mice and SJL/J mice were purchased from Japan SLC (Shizuoka, Japan) and Charles River Japan (Kanagawa, Japan), respectively. All mice were fed with standard laboratory chow and water ad libitum, and housed in specific pathogen-free conditions in the animal facility of Kyoto University. All experiments were performed with female mice at 8–12 weeks of age according to the protocol approved by the Animal Protection Committee of our institution.

Preparation of thioglycollate-elicited peritoneal macrophages

SR-PSOX/CXCL16 KO and WT mice were injected intraperitoneally with 3 ml of 3% thioglycollate (Eiken Chemical Co., Tokyo, Japan) and peritoneal exudate cells (PECs) were harvested 4 days later. Cells were cultured with complete RPMI medium (RPMI 1640 medium (Gibco BRL, Eggenstein, Germany) supplemented with 10% heat-inactivated fetal bovine serum, 100 μg/ml streptomycin (Sigma Chemical Co., St Louis, Missouri, USA) and 100 μg/ml penicillin (Sigma Chemical Co.)) for 2 h and, after removal of non-adherent cells, adherent PECs were cultured as peritoneal macrophages. Adherent PECs were resuspended and adjusted to a concentration of 1×10^6 cells/ml.

Preparation of caecal bacterial lysates (CBLs)

CBLs were prepared directly from the caecal contents of SR-PSOX/CXCL16 KO and WT mice according to a protocol described by Cong *et al*.[23] The sterility of the lysates was confirmed by culture.

Phagocytosis assay

The ex vivo phagocytosis assay was performed using pHrodo *Escherichia coli* BioParticles conjugate for phagocytosis (Invitrogen) according to the manufacturer's instructions. The fluorescence intensity was measured using a microplate reader (Fluoroskan Ascent FL: Labsystems, Helsinki, Finland) at the indicated times. For fluorescence microscopic observation of phagocytosis, peritoneal macrophages were seeded at 3×10^5 cells/well in 8-well Lab-Tek chamber glass slides (NUNC Roskilde, Denmark) and incubated overnight in complete medium. The wells were washed with phosphate-buffered saline (PBS), fluorescent particles were added and the slides were observed using fluorescence microscopy (Olympus, Tokyo, Japan) at the indicated times.

Stimulation and cytokine production assay of peritoneal macrophages

Peritoneal macrophages were seeded at 2.5×10^5 cells/well in 48-well culture plates and incubated overnight in complete medium. Cells were primed with 500 U/ml interferon γ (IFNγ; R&D Systems, Minneapolis, Minnesota, USA) for 16 h and then stimulated with 100 ng/ml lipopolysaccharide (LPS (L5668-2ML); Sigma Chemical Co.) or 30 μg/ml CBL for 24 h. The supernatants were collected and subjected to analysis of cytokine production by ELISA.

Induction of experimental colitis

DSS-colitis was induced in SR-PSOX/CXCL16 KO mice, WT littermates and C57BL/6 mice using a modification of the method described by Inoue *et al*.[24] In brief, to induce colitis, 3% DSS (molecular mass, 36–50 kDa; MP Biomedicals, Solon, Ohio, USA) in regular drinking water was administered for 5 days (from day 0 to 4), and then regular drinking water was given from day 5. Normal control mice received regular drinking water throughout the experiment. The mice were sacrificed on day 8 or day 14 to evaluate the acute inflammatory phase or the restitution phase, respectively. TNBS-colitis was induced in SJL/J mice using a modification of the method described by Neurath *et al*.[25]

The neutralising effect of mAb to SR-PSOX/CXCL16 on colitis models

To investigate the effect of blocking SR-PSOX/CXCL16 on experimental colitis, C57BL/6 mice with DSS-induced colitis and SJL/J mice with TNBS-induced colitis were injected intraperitoneally with 500 μg of mAb to SR-PSOX/CXCL16[26] dissolved in 200 μl of PBS or an equal amount of control rat immunoglobulin G (IgG) (MP Biomedicals) in PBS once a day from days 1 to 7 and days 1 to 3, respectively.

Microscopic assessment of colitis

The colonic tissues were treated using the same method as in Matsuura *et al*[27] and then analysed histologically in a blind manner. Histological damage of DSS- and TNBS-induced colitis was quantified using the histological scoring system described by Williams *et al*[28] and Elson *et al*,[29] respectively.

Colon fragment culture

Fragment culture of distal colon segments was performed according to the published method.[30] Culture supernatants were collected and stored at −80°C until assayed.

Isolation and stimulation of mesenteric lymph node (MLN) cells

MLNs were isolated as described previously.[31] MLN cells (2×10^5 cells/well) were incubated with immobilised anti-CD3 (5 μg/ml antimouse CD3ε; BD Pharmingen, San Diego, California, USA) plus CD28 (2 μg/ml antimouse CD28, BD Pharmingen) in 200 μl of complete medium containing 5×10^{-5} M 2-mercaptoethanol (Sigma Chemical Co.) in a 5% CO_2 incubator at 37°C for 72 h. The supernatant of the culture medium was collected and stored at −80°C until assayed.

Isolation of colonic lamina propria macrophages

Lamina propria macrophages were isolated using a modified protocol as described previously.[4] Briefly, mice were sacrificed, and colonic tissues were removed, washed with cold PBS and cut into three pieces. The resected colonic tissues were shaken with Hanks' balanced salt solution (HBSS; Gibco) for 1 min at 2800 rpm in a Mini Bead Beater (Biospec Products, Bartlesville, Oklahoma, USA) to remove faeces and mucus, dissected into small pieces and then incubated with HBSS containing 5% fetal calf serum and 5 mM EDTA (Gibco) for 30 min at 37°C under rotation at 120 rpm. After washing, the pieces were incubated with complete RPMI medium containing 1 mg/ml collagenase type II (Invitrogen, Carlsbad, California, USA), 1 mg/ml dispase (Gibco) and 40 μg/ml DNase (Roche, Mannheim, Germany) for 60 min at 37°C under rotation at 120 rpm to digest colonic tissues. After washing, the extracted cells were filtered and subjected to a magnetic cell separation system (Miltenyi Biotec, Auburn, California, USA) with antimouse CD11b microbeads to separate colonic lamina propria macrophages. Cell viability was determined by trypan blue staining, and >95% purity was confirmed by flow cytometry.

ELISA

The serum level of SR-PSOX/CXCL16 in the human subjects was determined quantitatively using a human CXCL16 immunoassay ELISA kit (R&D Systems). In the mouse model, the levels of SR-PSOX/CXCL16 in the serum and the supernatant of the colon fragment culture were measured using a mouse CXCL16 ELISA kit (R&D Systems). The cytokine levels of interleukin 6 (IL-6) and IL-12/23 p40 in the supernatants of the culture medium of thioglycollate-elicited peritoneal macrophage were measured using mouse ELISA kits (eBioscience, San Diego, California, USA). The secretions of IFNγ and IL-17 into the supernatants of culture medium in activated MLN cells were determined by mouse ELISA kits (eBioscience).

Quantitative analysis of gene expression of SR-PSOX/CXCL16 in colonic tissue

mRNA was assessed using colonic tissues isolated from the distal colon of WT mice with or without DSS-induced colitis. The extraction of total RNA, generation of cDNA and real-time reverse transcription–PCR (RT–PCR) were performed as described previously.[31] The following primers were used: SR-PSOX/CXCL16, 5′-GGCTTTGGACCCTTGTCTCTTG-3′ (forward) and 5′-TTGCGCTCAAAGCAGTCCACT-3′ (reverse); and glyceraldehyde phosphate dehydrogenase (GAPDH), 5′-CAA CTTTGTCAAGCTCATTTCC-3′ (forward) and 5′-GGTCCAG GGTTTCTTACTCC-3′ (reverse).

Western blot analysis

Colonic tissues were lysed in RIPA buffer (1% Triton X-100, 0.5% Na-deoxycholate, 0.1% sodium dodecyl sulfate (SDS), 20 mmol/l Tris–HCl (pH 7.4)) with protease inhibitor cocktail (Sigma Chemical Co.), and the insoluble material was removed by centrifugation at 12 000 *g* for 5 min at 4°C. The supernatants were boiled in sample buffer (0.05 mol/l Tris–HCl, 2% SDS, 6% β-mercaptoethanol, 10% glycerol, 1.25% bromophenol blue),

Gut 2011;**60**:1494–1505. doi:10.1136/gut.2010.221879

subjected to SDS–PAGE (10% polyacrylamide gels) and transferred onto polyvinylidine fluoride membranes (PALL Corporation, Pensacola, Florida, USA). The membranes were blocked with blocking buffer (Tris-buffered saline with 0.5% Tween-20 (TBS-T) containing 5% milk powder) and then incubated with a 1:1000 dilution of anti-CXCL16 mAb and with 1:5000 dilution

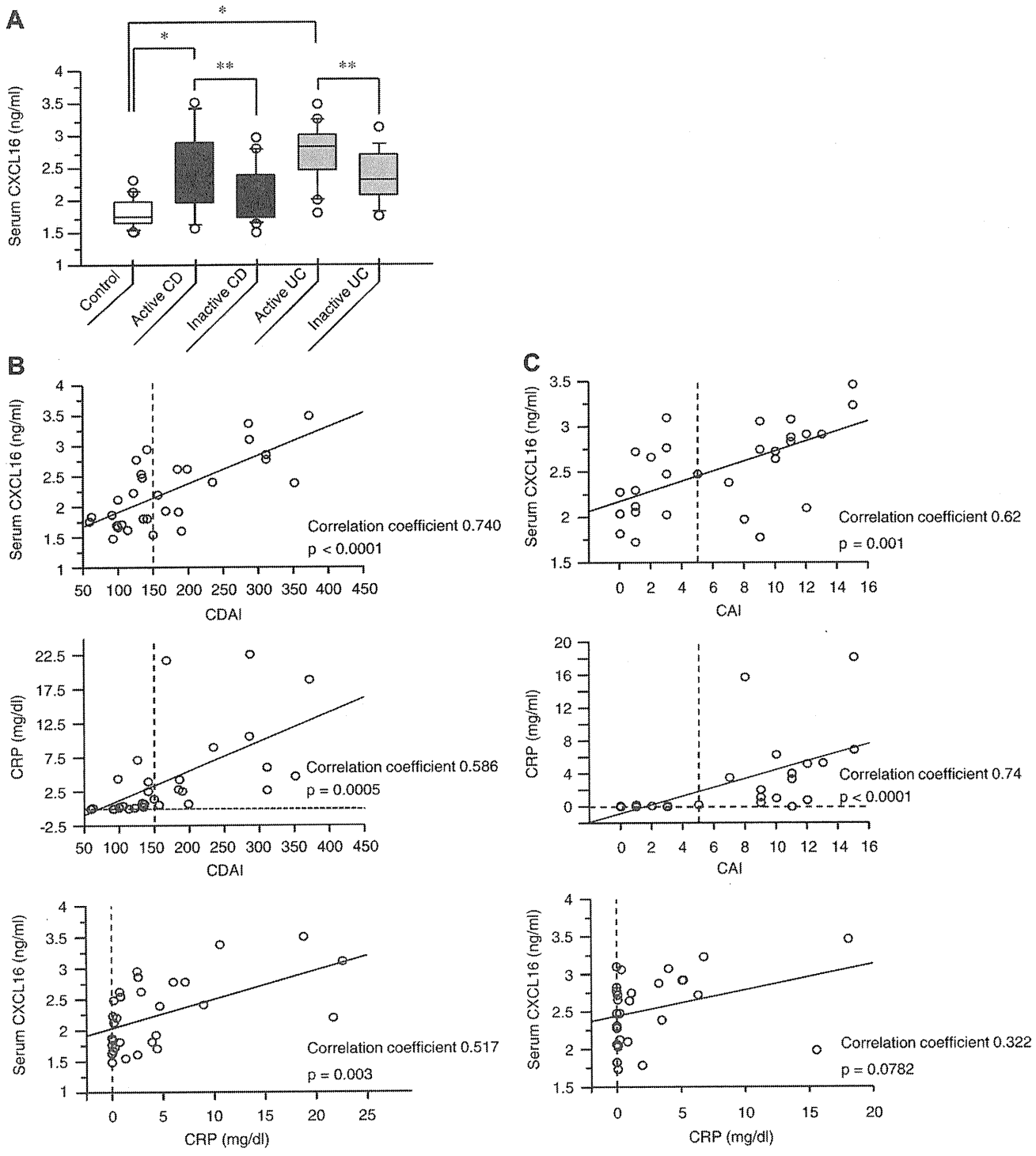

Figure 1 Serum levels of human SR-PSOX/CXCL16 are higher in patients with active inflammatory bowel disease (IBD). Serum samples were obtained from patients with active Crohn's diease (CD) (n=14), inactive CD (n=16), active ulcerative colitis (UC) (n=16) and inactive UC (n=13), and from healthy controls (n=16). Results are expressed as means±SEM. *p<0.05 compared with control and **p<0.05 between patients with active IBD and inactive IBD. (A) The statistical difference of serum SR-PSOX/CXCL16 in patients with IBD and healthy controls was determined by unpaired Student t test. (B) The relationship among serum SR-PSOX/CXCL16, C-reactive protein (CRP) and Crohn's Disease Activity Index (CDAI) in patients with CD was assessed by the Pearson correlation coefficient test. (C) The relationship among serum SR-PSOX/CXCL16, CRP and Clinical Activity Index (CAI) in patients with UC was investigated by the Pearson correlation coefficient test or Spearman correlation test.

of anti-β-actin mAb (Sigma Chemical Co.) overnight at 4°C. The membranes were washed and incubated with a horseradish peroxidase (HRP)-conjugated IgG. The immunoreactive bands were visualised with Immobilon Western chemiluminescent HRP substrate (Millipore, Billerica, Massachusetts, USA), and the images were recorded using a chemiluminescent image reader (LAS-3000; Fujifilm, Tokyo, Japan).

Immunohistochemistry

For SR-PSOX/CXCL16 immunostaining, colonic tissues of WT mice with or without DSS-induced colitis, and Peyer's patches as the positive control, were prepared as described previously.[24] The sections were incubated with biotinylated anti-CXCL16 antibody (1:250; R&D Systems) or goat IgG isotype control overnight at 4°C. After washing, the sections were incubated with

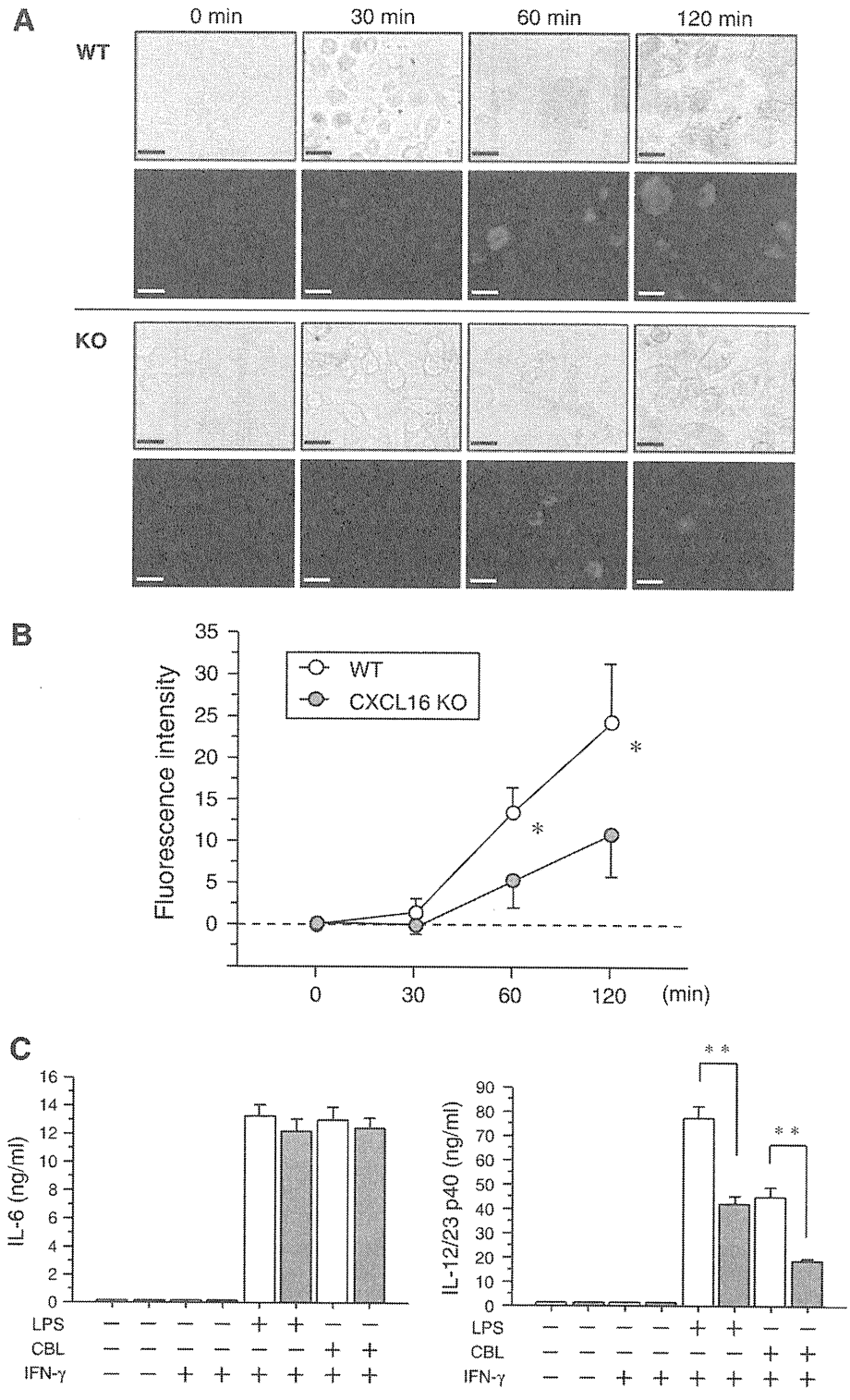

Figure 2 SR-PSOX/CXCL16 plays a role in phagocytosis of bacterial components and the production of interleukin 12 (IL-12) by macrophages. Thioglycollate-elicited peritoneal macrophages from SR-PSOX/CXCL16 knockout (KO) and wild-type (WT) mice were subjected to an ex vivo phagocytosis assay against bacteria. (A) Microscopic observation of phagocytosis was performed in peritoneal macrophages from WT mice (upper column) and SR-PSOX/CXCL16 KO mice (lower column). The upper and lower panels of each column show light microscopic findings and fluorescent images, respectively. Scale bars, 25 μm. (B) Fluorescence intensity, from which the fluorescence values of the no-cell background control wells were subtracted, was measured using a microplate reader at the indicated times. The statistical comparison of fluorescence intensity between WT (open circles) and SR-PSOX/CXCL16 KO macrophages (filled circles) was assessed by repeated measure analysis of variance followed by unpaired Student t test. (C) Peritoneal macrophages from WT (open bars) and SR-PSOX/CXCL16 KO mice (filled bars) were incubated with 500 U/ml interferon γ (IFNγ) for 16 h, followed by stimulation with 100 ng/ml lipopolysaccharide (LPS) or 30 μg caecal bacterial lysate (CBL) for 24 h, and the culture supernatants were analysed by ELISA to measure the concentrations of IL-6 and IL-12/23 p40. The results are expressed as means±SEM of the data from three independent experiments. The statistical difference was determined by unpaired Student t test. *p<0.05 and **p<0.01 between SR-PSOX/CXCL16 KO and WT macrophages.

Gut 2011;60:1494–1505. doi:10.1136/gut.2010.221879

streptavidin–HRP (1:1000; PerkinElmer, Waltham, Massachusetts, USA), treated with a tyramide signal amplification (TSA) biotin system (PerkinElmer), visualised with 3, 3'-diaminobenzidine tetrahydrochloride and counterstained with haematoxylin solution (Wako Pure Chemical, Osaka, Japan).

For immunofluorescence co-staining, cryosections (6 μm) of colonic tissue were fixed in cold acetone for 2 min and blocked with the Biotin Block system (DakoCytomation, Carpinteria, California, USA), Protein Block Serum-Free (DakoCytomation) and anti-CD16/32 mAb (1:500; eBioscience) to block endogenous biotin binding, non-specific protein binding and non-specific Fc binding, respectively. The sections were incubated with fluorescein isothiocyanate (FITC)-conjugated anti-CD11b mAb (1:200; BD Pharmingen) and biotinylated anti-CXCL16 antibody (1:1000; R&D Systems) or goat IgG isotype control overnight at 4°C. After quenching, the sections were incubated with streptavidin–HRP (1:1000). The signals were enhanced using the TSA biotin system (PerkinElmer) according to the manufacturer's protocol and finally visualised by Alexa 594-conjugated streptavidin (1:2000; Invitrogen).

Furthermore, to evaluate the difference in cells recruited to colonic tissues of SR-PSOX/CXCL16 KO and WT mice with or without DSS-induced colitis, colonic tissues were incubated with FITC-conjugated CD3 (1:200), CD11b (1:100) and CD11c (1:100) (eBioscience), followed by nuclear counterstaining with 4`,6-diamidino-2-phenylindole (DAPI; 1:10000). Mean numbers of cells recruited to colonic tissues from five different microscopic fields under high power (×400) were calculated in each mouse, and means ± SEM from six mice of each group are shown. Images were recorded using a fluorescence microscope (Olympus).

Fluorescence in situ hybridisation (FISH)

The universal eubacterial oligonucleotide probe EUB-338 (5'-GCT GCC TCC CGT AGG AGT-3') was synthesised and the 5' end was labelled with carbocyanite dye (Cy5). The sections (4 μm thick) were deparaffinised and incubated with 50 ng of oligonucleotide probe in 10 μl of hybridisation buffer (containing 20% formamide, 0.9 M NaCl, 20 mM Tris–HCl (pH 7.2), 0.01% SDS) in a humid chamber overnight at 46°C. After washing with the same buffer, nuclear counterstaining was performed with DAPI (0.04 μg/ml). Slides were visualised by fluorescence microscopy with a Leica CW4000 system (Leica, Wetzlar, Germany).

Statistical analysis

All numerical data are expressed as means±SEM. The differences between groups were analysed by unpaired Student t test, Mann–Whitney U test and analysis of variance (ANOVA) for repeated measures. Parametric and non-parametric correlation was examined by the Pearson correlation coefficient test and the Spearman correlation test, respectively. The cumulative survival rate was calculated by the Kaplan–Meier method, and survival curves were compared by log-rank test. A p value <0.05 was considered significant.

RESULTS

Serum levels of SR-PSOX/CXCL16 increase in patients with active IBD

The serum levels of SR-PSOX/CXCL16 were significantly higher in patients with active CD and UC than in control subjects. The serum levels of SR-PSOX/CXCL16 were also significantly higher in patients with active CD and UC than in those with inactive CD and UC, respectively (figure 1A). Also, the serum levels of SR-PSOX/CXCL16 significantly correlated with clinical activities of both CD and UC (CADI and CAI; figure 1B,C). Considering the relationship among SR-PSOX/CXCL16, C-reactive protein (CRP) and clinical activities in CD and UC, SR-PSOX/CXCL16 might be a more suitable marker reflecting the disease activity of CD compared with that of UC.

SR-PSOX/CXCL16 plays a role in phagocytosis of bacterial components

SR-PSOX/CXCL16 is reported to be a chemokine expressed specifically on APCs such as macrophages and dendritic cells.[11–13] In particular, we focused on macrophages that play a critical role in the uptake of luminal antigens and examined the ability of macrophages from SR-PSOX/CXCL16 KO and WT mice to phagocytose bacteria ex vivo. Fluorescence microscopy showed that the uptake of *E coli* by macrophages from both SR-PSOX/CXCL16 KO mice and WT mice increased in a time-dependent manner (figure 2A). Measurement of fluorescence intensity revealed that the fluorescence value was significantly lower from 60 to 120 min in SR-PSOX/CXCL16 KO macrophages than in WT macrophages (figure 2B).

SR-PSOX/CXCL16 is involved in the production of IL-12 by macrophages

To compare cytokine production by macrophages between SR-PSOX/CXCL16 KO and WT mice, we measured the levels of IL-6 and IL-12/23 p40 in the supernatant from macrophages of mice stimulated with LPS or CBL after pretreatment with IFNγ. There was no difference in the production of IL-6 by macrophages between SR-PSOX/CXCL16 KO and WT mice. In contrast, the production of IL-12/23 p40 by macrophages was

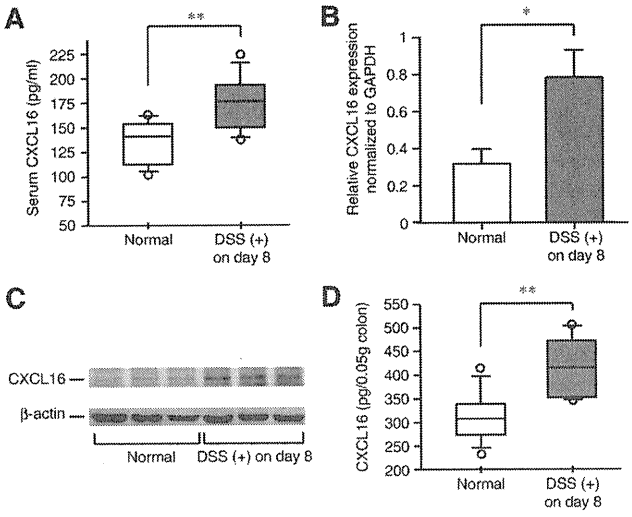

Figure 3 SR-PSOX/CXCL16 levels are higher in mice with dextran sulfate sodium (DSS)-induced colitis. (A) The serum levels of SR-PSOX/CXCL16 in mice with DSS-induced colitis on day 8 and control mice were measured by ELISA. (B). The gene expression of SR-PSOX/CXCL16 in colonic tissues with or without DSS-induced colitis was determined by quantitative real-time reverse transcription–PCR (RT–PCR) and was normalised to glyceraldehyde phosphate dehydrogenase (GAPDH). (C). The production of SR-PSOX/CXCL16 in colonic tissues with or without DSS-induced colitis was investigated by western blot analysis. (D) SR-PSOX/CXCL16 concentrations in supernatants of colon fragment cultures were measured by ELISA. The results are expressed as means±SEM (n=10 in each group). (A), (B) and (D) The statistical difference was determined by unpaired Student t test. *$p<0.05$ and **$p<0.01$ between mice with DSS-induced colitis and normal controls.

significantly lower in SR-PSOX/CXCL16 KO mice than in WT mice (figure 2C). We also observed a significant difference in IL-12/23 p40 production by macrophages between SR-PSOX/CXCL16 KO and WT mice even without pretreatment with IFNγ (data not shown).

Expression of SR-PSOX/CXCL16 increases in mice with DSS-induced colitis

Next, we investigated the in vivo expression of SR-PSOX/CXCL16 in the DSS-induced colitis model. The serum levels of SR-PSOX/CXCL16 were significantly higher in mice with DSS-induced colitis than in normal controls (figure 3A). To examine whether the expression of SR-PSOX/CXCL16 increases in inflamed tissues, we analysed the colonic tissues of mice with or without DSS-induced colitis. The gene expression of SR-PSOX/CXCL16 was significantly higher in colonic tissues of DSS-induced colitis than in normal colon (figure 3B). Western blot analysis and ELISA also revealed that SR-PSOX/CXCL16 expression was significantly higher in colonic tissues of DSS-induced colitis than in normal colon (figure 3C,D).

To identify the cells that mainly express SR-PSOX/CXCL16 in colonic tissues, we performed immunohistochemical analysis and immunofluorescent co-staining. The follicular-associated epithelia of Peyer's patches, used as a control, were positive for SP-PSOX/CXCL16, as reported previously (figure 4A, right upper panel).[32] SR-PSOX/CXCL16-expressing cells were increased markedly in colonic tissues of mice with DSS-induced colitis compared with normal colons, and these cells were observed from the mucosae to the submucosa (figure 4A, right lower panel). Immunofluorescent images revealed that SR-PSOX/CXCL16-expressing cells were mainly CD11b-positive cells (figure 4B).

Activity of DSS-induced colitis is reduced in SR-PSOX/CXCL16 KO mice

To investigate the role of SR-PSOX/CXCL16 in colonic inflammation, we compared SR-PSOX/CXCL16 KO and WT mice with DSS-induced colitis. Before the analysis, we confirmed that there was no difference in the subsets of lymphocytes between SR-PSOX/CXCL16 KO mice and WT mice in the static state (Supplementary figure 1 online). The amount of body weight

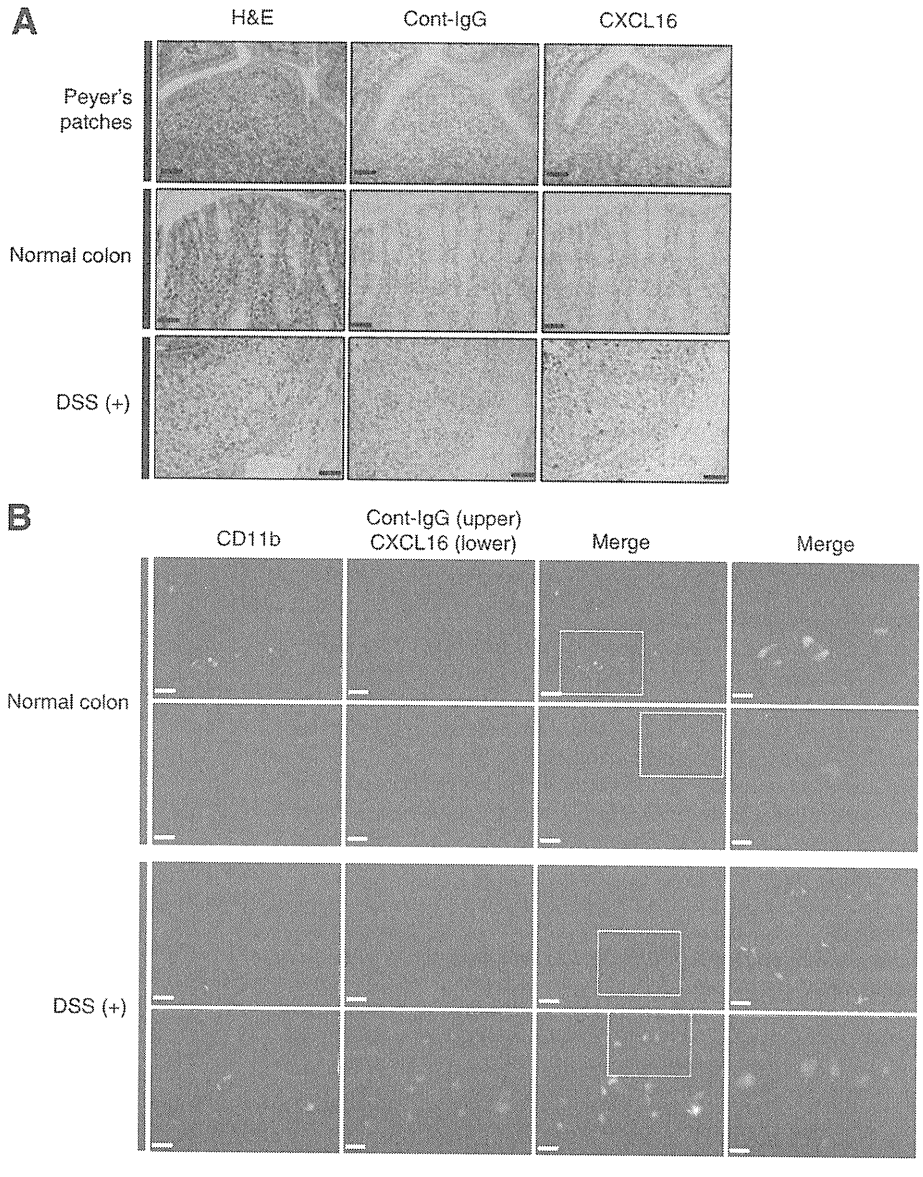

Figure 4 SR-PSOX/CXCL16 is expressed predominantly on macrophages in colonic tissues of mice with dextran sulfate sodium (DSS)-induced colitis. (A) Immunostaining was performed in Peyer's patches as a positive control, normal colons and colons with 3% DSS-induced colitis. Serial sections of each tissue were stained with H&E, control goat immunoglobulin G (IgG) and anti-mouse SR-PSOX/CXCL16 monoclonal antibody. (B). Immunofluorescent staining was performed in normal colons and colons with 3% DSS-induced colitis using antibodies against CD11b (green), SR-PSOX/CXCL16 (red) and control goat IgG. The merged images and their magnified images are shown. Scale bars, 50 μm (A), 20 μm (B, left 3 lanes) and 10 μm (B, right lane).

Gut 2011;**60**:1494–1505. doi:10.1136/gut.2010.221879

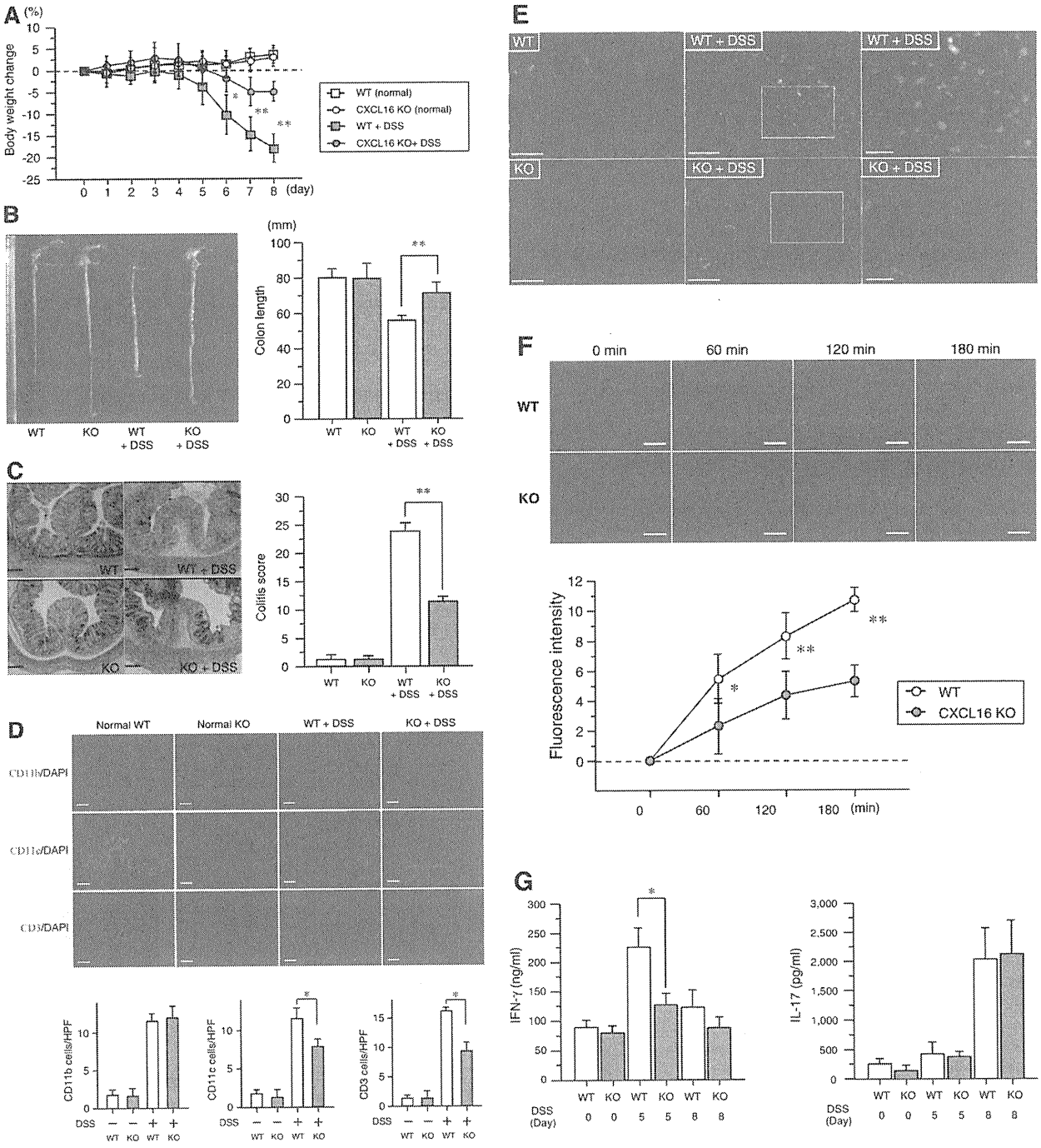

Figure 5 Activity of dextran sulfate sodium (DSS)-induced colitis is lower in SR-PSOX/CXCL16 knockout (KO) mice. (A) Serial change in body weight in SR-PSOX/CXCL16 KO and wild-type (WT) mice with or without 3% DSS-induced colitis. Data are expressed as the percentage change from the starting body weight. (B) Representative image and colonic length in SR-PSOX/CXCL16 KO and WT mice with or without 3% DSS-induced colitis on day 8. (C) Representative histological findings and the scores of colonic inflammation of SR-PSOX/CXCL16 KO and WT mice with or without 3% DSS-induced colitis on day 8. Scale bars, 100 μm. (D) Colonic tissues of SR-PSOX/CXCL16 KO and WT mice with or without 3% DSS-induced colitis were incubated with fluorescein isothiocyanate (FITC)-conjugated CD3, CD11b and CD11c, followed by nuclear counterstaining with 4′,6-diamidino-2-phenylindole (DAPI). Scale bars, 100 μm. (E) Fluorescent in situ hybridization analysis was performed with colonic tissues of SR-PSOX/CXCL16 KO and WT mice with or without 3% DSS-induced colitis using eubacterial oligonucleotide probe EUB-338 (red), followed by DAPI (blue). Scale bars, 50 μm (left two lanes) and 20 μm (right lane). (F) Colonic macrophages from SR-PSOX/CXCL16 KO and WT mice were subjected to an ex vivo phagocytosis assay against bacteria. Scale bars, 25 μm. (G) MLN cells from SR-PSOX/CXCL16 KO and WT mice on days 0, 5 and 8 after administration of 3% DSS were cultured with immobilised anti-CD3 plus CD28. Supernatants were collected after 72 h and subjected to ELISA to measure the concentration of interferon γ (IFNγ) and interleukin 17 (IL-17). (A)—(D), (F) and (G) The results are expressed as means±SEM (n=10—12 in each group). The statistical comparison was assessed by repeated measure analysis of variance followed by unpaired Student t test (A) and (F). The statistical difference was determined by unpaired Student t test (B), (D) and (G) or Mann—Whitney U test (C). *p<0.05 and **p<0.01 between SR-PSOX/CXCL16 KO mice and WT mice with DSS-induced colitis.

loss was significantly less in SR-PSOX/CXCL16 KO mice than in WT mice from 6 to 8 days after DSS administration (figure 5A). The colon was significantly longer in SR-PSOX/CXCL16 KO mice with DSS-induced colitis than in WT mice with DSS-induced colitis (figure 5B). The histological findings on day 8 after DSS administration in WT mice revealed severe epithelial destruction, remarkable infiltration of inflammatory cells with submucosal oedema, and crypt loss (figure 5C, right upper panel). In contrast, these findings were mild in SR-PSOX/CXCL16 KO mice (figure 5C, right lower panel). The total colitis score was significantly lower in SR-PSOX/CXCL16 KO mice with DSS-induced colitis than in WT mice with DSS-induced colitis (figure 5C). Furthermore, fluorescent immunohistochemistry showed that the numbers of CD11c- and CD3-positive cells were significantly lower in colonic tissues of SR-PSOX/CXCL16 KO mice with DSS-induced colitis than in WT mice with DSS-induced colitis, despite no significant difference of the number of CD11b-positive cells between these two groups (figure 5D).

SR-PSOX/CXCL16 is involved in bacterial invasion and phagocytosis of bacterial components in inflamed colonic tissues

FISH with a universal oligonucleotide probe was performed to elucidate the difference in bacterial invasion of colonic tissues between SR-PSOX/CXCL16 KO and WT mice with/without colitis. FISH analysis showed that fewer bacteria invaded colonic tissues in SR-PSOX/CXCL16 KO mice with colitis compared with WT mice with colitis (figure 5E). Additionally, we investigated the phagocytic activity of colonic macrophages. Similar to the data with peritoneal macrophages, the fluorescence value was significantly lower from 60 to 180 min in SR-PSOX/CXCL16 KO colonic macrophages than in WT colonic macrophages (figure 5F).

SR-PSOX/CXCL16 is related to the Th1 but not Th17 immune response in DSS-induced colitis

Next, we measured cytokine production by MLN cells from both SR-PSOX/CXCL16 KO and WT mice with DSS-induced colitis. The production of IFNγ on day 5 after DSS administration was significantly lower in SR-PSOX/CXCL16 KO mice than in WT mice (figure 5G). In contrast, the production of IL-17 did not differ significantly between SR-PSOX/CXCL16 KO and WT mice with DSS-induced colitis throughout the experiment (figure 5G).

Administration of SR-PSOX/CXCL16 mAb attenuates experimental murine colitis

To assess the neutralising effect of a mAb to SR-PSOX/CXCL16 in mice with colonic inflammation, we analysed two experimental murine colitis models: DSS-induced colitis as an epithelial injury model and TNBS-induced colitis as a Th1-mediated colitis model.[33] The body weight of mice with DSS-colitis treated with control IgG decreased and reached the lowest level on day 9, and gradually increased thereafter, although complete recovery was not obtained even on day 14. In contrast, in mice treated with SR-PSOX/CXCL16 mAb the body weight

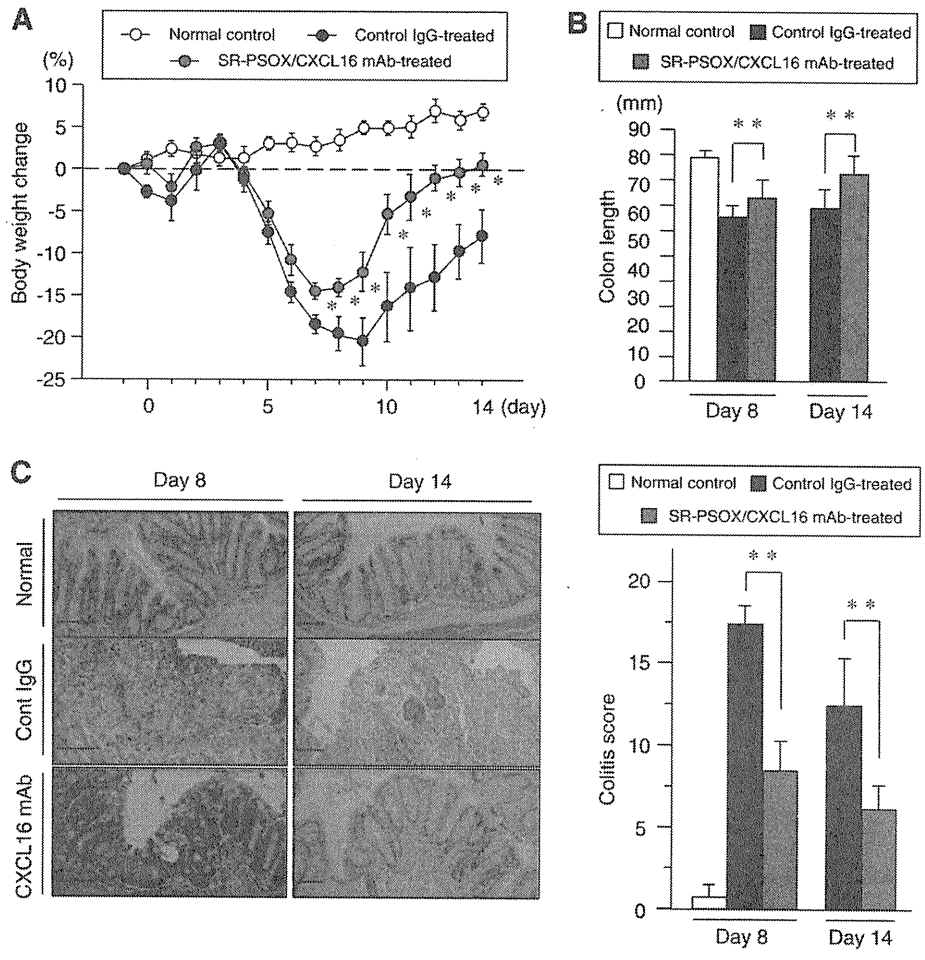

Figure 6 Administration of SR-PSOX/CXCL16 monoclonal antibody (mAb) attenuates dextran sulfate sodium (DSS)-induced colitis. A 500 μg aliquot of SR-PSOX/CXCL16 mAb or an equal amount of control rat immunoglobulin (IgG) was administered to C57BL/6 mice with 3% DSS-induced colitis by intraperitoneal injection once a day from day 1 to day 7. (A) Serial change in body weight in normal control mice (open circles), control IgG-treated mice with DSS-induced colitis (filled circles) and SR-PSOX/CXCL16 mAb-treated mice with DSS-induced colitis (grey circles). The data are expressed as the percentage change from the starting body weight. (B) Colonic length on day 8 and day 14 after administration of DSS. (C) Representative histological findings and the scores of colonic inflammation on day 8 and day 14. Scale bars, 100 μm. The results are expressed as means±SEM (n=12 in each group). (A) The statistical comparison was assessed by repeated measure analysis of variance followed by unpaired Student t test. (B) and (C) The differences of colon length and colitis score between the groups were determined by unpaired Student t test and Mann–Whitney U test, respectively. *p<0.05 and **p<0.01 between SR-PSOX/CXCL16 mAb-treated and control IgG-treated mice with DSS-induced colitis.

Gut 2011;**60**:1494–1505. doi:10.1136/gut.2010.221879

decreased to the lowest level on day 7 and recovered to a level similar to that before DSS administration on day 14. The body weight of mice treated with SR-PSOX/CXCL16 mAb was significantly higher from day 7 to 14 than that of IgG-treated control mice (figure 6A). Furthermore, administration of SR-PSOX/CXCL16 mAb significantly attenuated the shortening of colonic length (figure 6B), and significantly reduced colonic damage and the colitis score of mice with DSS-induced colitis on both day 8 and day 14 (figure 6C).

In addition, in TNBS-induced colitis, administration of SR-PSOX/CXCL16 mAb significantly ameliorated the body weight change on day 4 (figure 7A). Histological findings showed severe epithelial destruction, marked infiltration of inflammatory cells with mucosal oedema and remarkable loss of cryptal cells in control IgG-treated mice. In contrast, these colonic inflammatory findings were attenuated in SR-PSOX/CXCL16 mAb-treated mice. The colitis score was significantly lower in SR-PSOX/CXCL16 mAb-treated mice than in control IgG-treated mice (figure 7B). Furthermore, the overall survival rate of mice with TNBS-induced colitis treated with SR-PSOX/CXCL16 mAb was significantly higher than that of control IgG-treated mice (78.7% vs 38.9%; p=0.04; figure 7C).

DISCUSSION

Recent genetic approaches for elucidating the pathogenesis of IBD revealed that abnormality of the genes related to the innate immune response by recognising and/or processing bacterial components is involved in the development of IBD.[34–37] Kamada *et al* suggested that the abnormal response of intestinal macrophages to commensal bacteria results in chronic intestinal inflammation.[4] Therefore, the control of the abnormal innate immune response of APCs to commensal bacteria is important in the treatment of IBD. Indeed, we showed that macrophage-targeting treatment ameliorates colonic inflammation in an experimental colitis model.[5] Taken together, targeting molecules related to macrophages appears to be a promising approach for the treatment of IBD. SR-PSOX/CXCL16 may be one such candidate molecule, because it is mainly expressed in APCs.

First, we found that the serum level of SR-PSOX/CXCL16 was significantly higher in patients with active IBD as reported previously,[38] and moreover that the level correlated with the disease activity in patients with IBD. Analysis of correlation between disease activity and SR-PSOX/CXCL16 or CRP suggests that the serum SR-PSOX/CXCL16 might be a suitable biomarker for evaluating disease activity of CD rather than UC.

Furthermore, we investigated the serum concentration and tissue expression of SR-PSOX/CXCL16 in mice with DSS-induced colitis. Similar to human IBD, the serum level of SR-PSOX/CXCL16 and its expression in colonic tissue was significantly higher in mice with DSS-induced colitis than in normal mice. In addition, SR-PSOX/CXCL16 was expressed mainly on CD11b-positive cells and markedly increased in the colonic mucosa of mice with DSS-induced colitis, although these cells were barely observed in the colonic mucosa under normal conditions. Previous reports have shown that several inflammatory cytokines including IFNγ, tumour necrosis factor α (TNFα) and IL-18 induce the expression of SR-PSOX/CXCL16.[39–41] Thus, increased concentration of various inflammatory cytokines in the inflamed colonic mucosa may contribute to enhanced expression of SR-PSOX/CXCL16 on macrophages.

Next, to evaluate the role of SR-PSOX/CXCL16 in both macrophage phagocytic activity and cytokine production, we examined phagocytosis and bacteria stimulated-cytokine

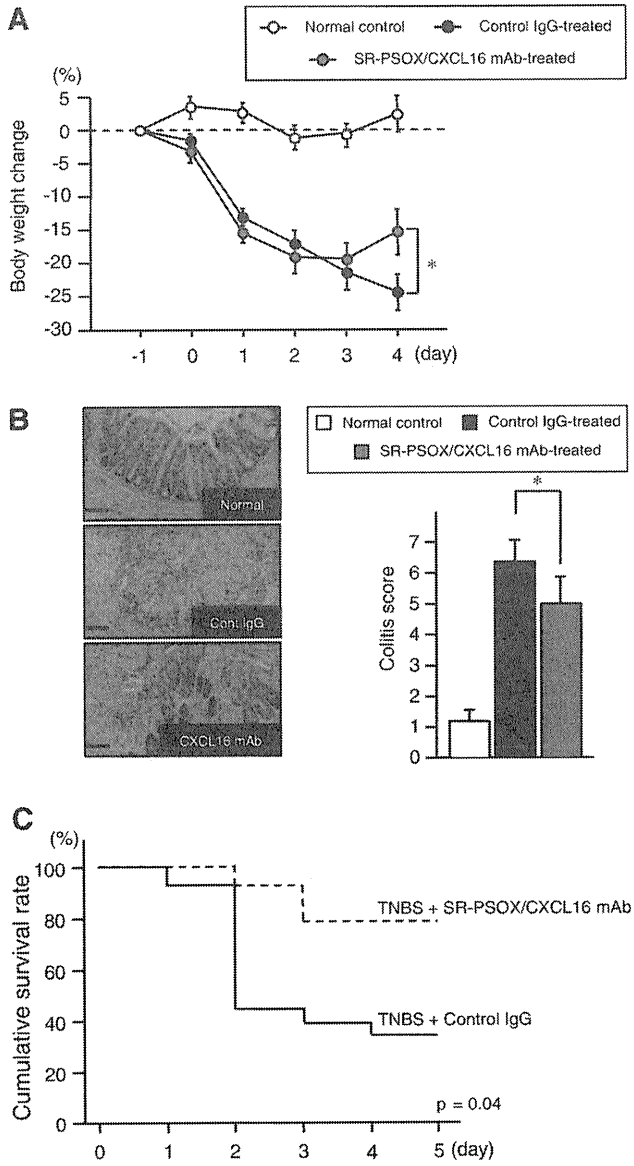

Figure 7 Administration of SR-PSOX/CXCL16 monoclonal antibody (mAb) attenuates trinitrobenzene sulfonic acid (TNBS)-induced colitis. A 500 μg aliquot of SR-PSOX/CXCL16 mAb or an equal amount of control rat immunoglobulin G (IgG) was given to SJL/J mice with TNBS-induced colitis by intraperitoneal injection once a day from day 1 to day 3. (A) Serial change in body weight in normal control mice (open circles), control IgG-treated mice with TNBS-induced colitis (filled circles) and SR-PSOX/CXCL16 mAb-treated mice with TNBS-induced colitis (grey circles). The data are expressed as the percentage change from the starting body weight. (B) Representative histological findings and the scores of colonic inflammation on day 4. Scale bars, 100 μm. The results are expressed as means±SEM (n=8 in each group). The difference of body weight change and colitis score between groups was assessed by repeated measure analysis of variance followed by unpaired Student t test and Mann–Whitney U test, respectively. *p<0.05 between SR-PSOX/CXCL16 mAb-treated and control IgG-treated mice with TNBS-induced colitis. (C) Cumulative survival rate of mice with TNBS-colitis treated with SR-PSOX/CXCL16 or control IgG was calculated by the Kaplan–Meier method, and survival curves were compared by log-rank test.

production in peritoneal macrophages from SR-PSOX/CXCL16 KO mice in vitro. Our data clearly demonstrated that both the phagocytic ability and IL-12 production of macrophages of

SR-PSOX/CXCL16 KO mice was significantly impaired. Of note, LPS- and CBL-induced IL-12 production was significantly reduced in SR-PSOX/CXCL16 KO mice in the presence of IFNγ. This appears reasonable, because IFNγ has been reported to enhance SR-PSOX/CXCL16 expression.[39]

The present study clearly showed that SR-PSOX/CXCL16 KO mice had reduced activity of DSS-induced colitis. Moreover, SR-PSOX/CXCL16 mAb ameliorated colitis in two different experimental models. These data indicate that SR-PSOX/CXCL16 plays important roles in the development of colitis. The DSS-induced colitis model is characterised by direct epithelial injury and subsequent activation of macrophages,[35] and SR-PSOX/CXCL16 is reported to be involved in DSS-induced IL-1β production by macrophages.[42] Therefore, the DSS-induced colitis model is suitable for investigating the interaction between luminal bacteria and macrophages expressing SR-PSOX/CXCL16. In our current study, SR-PSOX/CXCL16 was expressed predominantly on CD11b-positive cells at subepithelial sites of the inflamed colonic mucosa. In addition, we found that bacterial invasion of the lamina propria in the colitic mucosa was reduced in SR-PSOX/CXCL16 KO mice. SR-PSOX/CXCL16 has been reported to act as a scavenger receptor that mediates adhesion and phagocytosis of bacteria by APCs.[14] In this connection, we demonstrated here that both peritoneal and intestinal macrophages of SR-PSOX/CXCL16 KO mice had reduced ability to phagocytose bacterial antigens. Taken together, our data suggest that SR-PSOX/CXCL16 exerts its colitogenic action at least in part by promoting bacterial uptake into macrophages in the colonic mucosa.

In this study, SR-PSOX/CXCL16 mAb also ameliorated TNBS-induced colitis, a Th1-mediated colitis model. An interesting finding in this study is that SR-PSOX/CXCL16 KO macrophages had an impaired ability to produce IL-12 in response to not only LPS but also commensal bacterial antigens, although their production of IL-6 was unaffected. Moreover, we observed that MLN cells from SR-PSOX/CXCL16 KO mice with DSS-induced colitis showed reduced production of IFNγ but not of IL-17. Because IL-6 is essential for the induction of Th17 cells, the lack of difference in IL-6 production by macrophages or IL-17 production by MLN cells between SR-PSOX/CXCL16 KO and WT mice suggests that SR-PSOX/CXCL16 is not involved in the Th17-mediated immune response. Taken together, our data indicate that SR-PSOX/CXCL16 plays a colitogenic role by enhancing the Th1 immune response. Of note, IL-17A had a protective role in the $CD45RB^{hi}$ transfer model of colitis and suppressed the induction of T-bet in maturing Th1 cells.[43] Thus, targeting SR-PSOX/CXCL16 seems to be an ideal treatment for preventing Th1-mediated colitis, without affecting the IL-17-mediated immune response.

In conclusion, our present data clearly demonstrated that SR-PSOX/CXCL16 plays a critical role in the development of colonic inflammation probably by both activating uptake of commensal bacteria and enhancing the Th1 immune response. SR-PSOX/CXCL16 may be a therapeutic target for patients with IBD.

Funding This work was supported by a Grant-in-Aid for Scientific Research (C) from the Ministry of Culture and Science of Japan (grant 18590677), the Kato Memorial Trust for Nambyo Research, the Shimizu Foundation for the Promotion of Immunology Research and the Japan Foundation for Applied Enzymology to HN, Grant-in-Aids for Scientific Research (16017240, 16017249, 17013051, 17659212 and 18012029) from the Ministry of Education, Culture, Sports, Science, and Technology of Japan, Grant-in-Aid for Scientific Research (15209024 and 18209027) from JSPS and Grant-in-Aid for Research on Measures for Intractable Diseases, and Research on Advanced Medical Technology (nano005) from the Ministry of Health, Labor, and Welfare, Japan to TC.

Competing interests None.

Patient consent Obtained.

Ethics approval This study was conducted with the approval of the Kyoto University Hospital Ethics Committee.

Provenance and peer review Not commissioned; externally peer reviewed.

REFERENCES

1. **Podolsky DK.** Inflammatory bowel disease. *N Engl J Med* 2002;**347**:417–29.
2. **Cho JH.** The genetics and immunopathogenesis of inflammatory bowel disease. *Nat Rev Immunol* 2008;**8**:458–66.
3. **Shih DQ,** Targan SR, McGovern D. Recent advances in IBD pathogenesis: genetics and immunobiology. *Curr Gastroenterol Rep* 2008;**10**:568–75.
4. **Kamada N,** Hisamatsu T, Okamoto S, *et al.* Abnormally differentiated subsets of intestinal macrophage play a key role in Th1-dominant chronic colitis through excess production of IL-12 and IL-23 in response to bacteria. *J Immunol* 2005;**175**:6900–8.
5. **Nakase H,** Okazaki K, Tabata Y, *et al.* Development of an oral drug delivery system targeting immune-regulating cells in experimental inflammatory bowel disease: a new therapeutic strategy. *J Pharmacol Exp Ther* 2000;**292**:15–21.
6. **Zlotnik A,** Yoshie O. Chemokines: a new classification system and their role in immunity. *Immunity* 2000;**12**:121–7.
7. **Sallusto F,** Mackay CR. Chemoattractants and their receptors in homeostasis and inflammation. *Curr Opin Immunol* 2004;**16**:724–31.
8. **Bromley SK,** Mempel TR, Luster AD. Orchestrating the orchestrators: chemokines in control of T cell traffic. *Nat Immunol* 2008;**9**:970–80.
9. **Zimmerman NP,** Vongsa RA, Wendt MK, *et al.* Chemokines and chemokine receptors in mucosal homeostasis at the intestinal epithelial barrier in inflammatory bowel disease. *Inflamm Bowel Dis* 2008;**14**:1000–11.
10. **Gijsbers K,** Geboes K, Van Damme J. Chemokines in gastrointestinal disorders. *Curr Drug Targets* 2006;**7**:47–64.
11. **Shimaoka T,** Kume N, Minami M, *et al.* Molecular cloning of a novel scavenger receptor for oxidized low density lipoprotein, SR-PSOX, on macrophages. *J Biol Chem* 2000;**275**:40663–6.
12. **Matloubian M,** David A, Engel S, *et al.* A transmembrane CXC chemokine is a ligand for HIV-coreceptor Bonzo. *Nat Immunol* 2000;**1**:298–304.
13. **Wilbanks A,** Zondlo SC, Murphy K, *et al.* Expression cloning of the STRL33/BONZO/TYMSTR ligand reveals elements of CC, CXC, and CX3C chemokines. *J Immunol* 2001;**166**:5145–54.
14. **Shimaoka T,** Nakayama T, Kume N, *et al.* Cutting edge: SR-PSOX/CXC chemokine ligand 16 mediates bacterial phagocytosis by APCs through its chemokine domain. *J Immunol* 2003;**171**:1647–51.
15. **Yamauchi R,** Tanaka M, Kume N, *et al.* Upregulation of SR-PSOX/CXCL16 and recruitment of CD8+ T cells in cardiac valves during inflammatory valvular heart disease. *Arterioscler Thromb Vasc Biol* 2004;**24**:282–7.
16. **Lehrke M,** Millington SC, Lefterova M, *et al.* CXCL16 is a marker of inflammation, atherosclerosis, and acute coronary syndromes in humans. *J Am Coll Cardiol* 2007;**49**:442–9.
17. **Wu T,** Xie C, Wang HW, *et al.* Elevated urinary VCAM-1, P-selectin, soluble TNF receptor-1, and CXC chemokine ligand 16 in multiple murine lupus strains and human lupus nephritis. *J Immunol* 2007;**179**:7166–75.
18. **Best WR,** Becktel JM, Singleton JW, *et al.* Development of a Crohn's disease activity index. National Cooperative Crohn's Disease Study. *Gastroenterology* 1976;**70**:439–44.
19. **Rachmilewitz D.** Coated mesalazine (5-aminosalicylic acid) versus sulphasalazine in the treatment of active ulcerative colitis: a randomised trial. *BMJ* 1989;**298**:82–6.
20. **Targan SR,** Hanauer SB, van Deventer SJ, *et al.* A short-term study of chimeric monoclonal antibody cA2 to tumor necrosis factor alpha for Crohn's disease. Crohn's Disease cA2 Study Group. *N Engl J Med* 1997;**337**:1029–35.
21. **Andus T,** Klebl F, Rogler G, *et al.* Patients with refractory Crohn's disease or ulcerative colitis respond to dehydroepiandrosterone: a pilot study. *Aliment Pharmacol Ther* 2003;**17**:409–14.
22. **Shimaoka T,** Seino K, Kume N, *et al.* Critical role for CXC chemokine ligand 16 (SR-PSOX) in Th1 response mediated by NKT cells. *J Immunol* 2007;**179**:8172–9.
23. **Cong Y,** Brandwein SL, McCabe RP, *et al.* CD4+ T cells reactive to enteric bacterial antigens in spontaneously colitic C3H/HeJBir mice: increased T helper cell type 1 response and ability to transfer disease. *J Exp Med* 1998;**187**:855–64.
24. **Inoue S,** Nakase H, Matsuura M, *et al.* The effect of proteasome inhibitor MG 132 on experimental inflammatory bowel disease. *Clin Exp Immunol* 2009;**156**:172–82.
25. **Neurath MF,** Fuss I, Kelsall BL, *et al.* Antibodies to interleukin 12 abrogate established experimental colitis in mice. *J Exp Med* 1995;**182**:1281–90.
26. **Shimaoka T,** Nakayama T, Fukumoto N, *et al.* Cell surface-anchored SR-PSOX/CXC chemokine ligand 16 mediates firm adhesion of CXC chemokine receptor 6-expressing cells. *J Leukoc Biol* 2004;**75**:267–74.
27. **Matsuura M,** Okazaki K, Nishio A, *et al.* Therapeutic effects of rectal administration of basic fibroblast growth factor on experimental murine colitis. *Gastroenterology* 2005;**128**:975–86.
28. **Williams KL,** Fuller CR, Dieleman LA, *et al.* Enhanced survival and mucosal repair after dextran sodium sulfate-induced colitis in transgenic mice that overexpress growth hormone. *Gastroenterology* 2001;**120**:925–37.

29. **Elson CO,** Beagley KW, Sharmanov AT, *et al.* Hapten-induced model of murine inflammatory bowel disease: mucosa immune responses and protection by tolerance. *J Immunol* 1996;**157**:2174–85.
30. **Sellon RK,** Tonkonogy S, Schultz M, *et al.* Resident enteric bacteria are necessary for development of spontaneous colitis and immune system activation in interleukin-10-deficient mice. *Infect Immun* 1998;**66**:5224–31.
31. **Mikami S,** Nakase H, Yamamoto S, *et al.* Blockade of CXCL12/CXCR4 axis ameliorates murine experimental colitis. *J Pharmacol Exp Ther* 2008;**327**:383–92.
32. **Hase K,** Murakami T, Takatsu H, *et al.* The membrane-bound chemokine CXCL16 expressed on follicle-associated epithelium and M cells mediates lympho-epithelial interaction in GALT. *J Immunol* 2006;**176**:43–51.
33. **Sartor RB.** Animal models of intestinal inflammation. In: Sartor RB, Sandborn WJ, eds. *Kirsner's Inflammatory Bowel Disease*. 6th edn. Edinburgh: Saunders, 2004:120–37.
34. **Hugot JP,** Chamaillard M, Zouali H, *et al.* Association of NOD2 leucine-rich repeat variants with susceptibility to Crohn's disease. *Nature* 2001;**411**:599–603.
35. **Ogura Y,** Bonen DK, Inohara N, *et al.* A frameshift mutation in NOD2 associated with susceptibility to Crohn's disease. *Nature* 2001;**411**:603–6.
36. **Hampe J,** Franke A, Rosenstiel P, *et al.* A genome-wide association scan of nonsynonymous SNPs identifies a susceptibility variant for Crohn's disease in ATG16L1. *Nat Genet* 2007;**39**:207–11.
37. **Parkes M,** Barrett JC, Prescott NJ, *et al.* Sequence variants in the autophagy gene IRGM and multiple other replicating loci contribute to Crohn's disease susceptibility. *Nat Genet* 2007;**39**:830–2.
38. **Lehrke M,** Konrad A, Schachinger V, *et al.* CXCL16 is a surrogate marker of inflammatory bowel disease. *Scand J Gastroenterol* 2008;**43**:283–8.
39. **Wuttge DM,** Zhou X, Sheikine Y, *et al.* CXCL16/SR-PSOX is an interferon-γ-regulated chemokine and scavenger receptor expressed in atherosclerotic lesions. *Arterioscler Thromb Vasc Biol* 2004;**24**:750–5.
40. **Abel S,** Hundhausen C, Mentlein R, *et al.* The transmembrane CXC-chemokine ligand 16 is induced by IFN-γ and TNF-α and shed by the activity of the disintegrin-like metalloproteinase ADAM10. *J Immunol* 2004;**172**:6362–72.
41. **Chandrasekar B,** Mummidi S, Valente AJ, *et al.* The pro-atherogenic cytokine interleukin-18 induces CXCL16 expression in rat aortic smooth muscle cells via MyD88, interleukin-1 receptor-associated kinase, tumor necrosis factor receptor-associated factor 6, c-Src, phosphatidylinositol 3-kinase, Akt, c-Jun N-terminal kinase, and activator protein-1 signaling. *J Biol Chem* 2005;**280**:26263–77.
42. **Kwon KH,** Ohigashi H, Murakami A. Dextran sulfate sodium enhances interleukin-1 beta release via activation of p38 MAPK and ERK1/2 pathways in murine peritoneal macrophages. *Life Sci* 2007;**81**:362–71.
43. **O'Connor W Jr,** Kamanaka M, Booth CJ, *et al.* A protective function for interleukin 17A in T cell-mediated intestinal inflammation. *Nat Immunol* 2009;**10**:603–9.

Editor's quiz: GI snapshot

Left lower quadrant abdominal pain caused by an IUCD

CLINICAL PRESENTATION

A previously healthy 42-year-old woman presented with mild left lower quadrant abdominal pain. There was no relevant medical or family history except she had a T-shaped copper intrauterine contraceptive device (IUCD) inserted 10 years previously. The remainder of her obstetric history was non-specific and included one normal vaginal delivery. Physical examination and laboratory findings at the time of presentation were unremarkable.

Plain radiographs of the abdomen identified the IUCD in the pelvic cavity (figure 1); however, the IUCD was not detected during gynaecological ultrasonography. Further abdominal CT scanning did not reveal any definite focal lesions and the IUCD was not identified (figure 2).

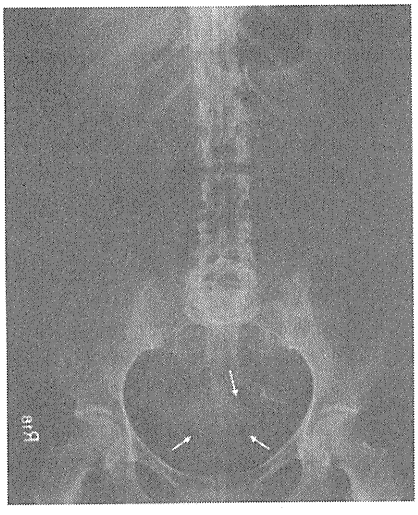

Figure 1 Plain abdominal radiograph showed the T-shaped intrauterine contraceptive device (IUCD) in the left pelvic cavity. The surrounding fat planes of the uterus were identified (arrows) and the device appeared separate from the fat planes.

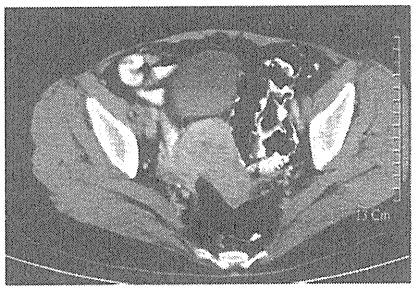

Figure 2 Contrast-enhanced CT scan using the soft tissue window setting did not identify any definite focal lesions.

QUESTION

What is your diagnosis?

What additional tests are indicated and how should the patient be managed?

See page 1562 for the answer

Huan-Lun Hsu,[1] Chin-Chen Chang,[2] Jin-Tung Liang,[3] Kao-Lang Liu[2]

[1]Department of Internal Medicine, Far Eastern Memorial Hospital, National Taiwan University Hospital and National Taiwan University College of Medicine, Taipei, Taiwan; [2]Departments of Medical Imaging, National Taiwan University Hospital and National Taiwan University College of Medicine, Taipei, Taiwan; [3]Department of Surgery, National Taiwan University Hospital and National Taiwan University College of Medicine, Taipei, Taiwan

Correspondence to Dr Kao-Lang Liu, Department of Medical Imaging, National Taiwan University Hospital, No. 7, Chung-Shan South Road, Taipei, Taiwan; lkl@ntu.edu.tw

Competing interests None.

Patient consent Obtained.

Provenance and peer review Not commissioned; externally peer reviewed.

Published Online First 4 March 2011

Gut 2011;**60**:1505. doi:10.1136/gut.2010.209486

Published OnlineFirst June 3, 2011; DOI:10.1158/1078-0432.CCR-10-3131

Clinical Cancer Research

The Efficacy of IGF-I Receptor Monoclonal Antibody against Human Gastrointestinal Carcinomas is Independent of *k-ras* Mutation Status

Masanori Ii, Hua Li, Yasushi Adachi, et al.

Clin Cancer Res 2011;17:5048-5059. Published OnlineFirst June 3, 2011.

Published OnlineFirst June 3, 2011; DOI:10.1158/1078-0432.CCR-10-3131

Cancer Therapy: Preclinical

Clinical Cancer Research

The Efficacy of IGF-I Receptor Monoclonal Antibody against Human Gastrointestinal Carcinomas is Independent of *k-ras* Mutation Status

Masanori Ii[1], Hua Li[1], Yasushi Adachi[1], Hiroyuki Yamamoto[1], Hirokazu Ohashi[1], Hiroaki Taniguchi[1], Yoshiaki Arimura[1], David P. Carbone[2,3], Kohzoh Imai[4], and Yasuhisa Shinomura[1]

Abstract

Purpose: Insulin-like growth factor (IGF)-I receptor (IGF-IR) signaling is required for carcinogenicity and proliferation of gastrointestinal cancers. We have previously shown successful targeting therapy for colorectal, pancreatic, gastric, and esophageal carcinomas using recombinant adenoviruses expressing dominant negative IGF-IR. Mutation in *k-ras* is one of key factors in gastrointestinal cancers. In this study, we sought to evaluate the effect of a new monoclonal antibody for IGF-IR, figitumumab (CP-751,871), on the progression of human gastrointestinal carcinomas with/without *k-ras* mutation.

Experimental Design: We assessed the effect of figitumumab on signal transduction, proliferation, and survival in six gastrointestinal cancer cell lines with/without *k-ras* mutation, including colorectal and pancreatic adenocarcinoma, esophageal squamous cell carcinoma, and hepatoma. Combination effects of figitumumab and chemotherapy were also studied. Then figitumumab was evaluated in the treatment of xenografts in nude mice.

Results: Figitumumab blocked autophosphorylation of IGF-IR and its downstream signals. The antibody suppressed proliferation and tumorigenicity in all cell lines. Figitumumab inhibited survival by itself and up-regulated chemotherapy (5-FU and gemcitabine) induced apoptosis. Moreover, the combination of this agent and chemotherapy was effective against tumors in mice. The effect of figitumumab was not influenced by the mutation status of *k-ras*. Figitumumab reduced expression of IGF-IR but not insulin receptor in these xenografted tumors. The drug did not affect murine body weight or blood concentrations of glucose, insulin, IGF binding protein 3, and growth hormone.

Conclusions: IGF-IR might be a good molecular therapeutic target and figitumumab may thus have therapeutic value in human gastrointestinal malignancies even in the presence of *k-ras* mutations. *Clin Cancer Res; 17(15); 5048–59. ©2011 AACR.*

Introduction

Gastrointestinal (GI) cancers encompass a variety of diseases, many of whose prognoses are poor. Although only colorectal cancer is listed in the top 10 for incidence rates of cancer in the USA, 4 GI cancers, including colorectal, pancreas, liver and the biliary tract, and esophageal, are in the top 10 for death rates from cancer (1). In Japan, there are 5 GI cancers, including colorectal, gastric, pancreatic, hepatic, and biliary tract, in the top 10 for death rates in 2007. Therefore, we must to seek new therapeutic options for GI cancers.

Signals from a variety of growth factors are required for tumorigenesis and cancer development in human malignancies (2, 3). Recently, advances in molecular cancer research have brought new therapeutic forces from the bench into clinic. One group of new targets is the receptor tyrosine kinases for which specific small molecule tyrosine kinase inhibitors (TKIs) or blocking monoclonal antibodies (mAbs) exist. Type I insulin-like growth factor (IGF)-I receptor (IGF-IR) could be the next important molecular target (3, 4).

Binding of the ligands, IGF-I and IGF-II, to IGF-IR causes receptor autophosphorylation and activates multiple signaling pathways, including the mitogen-activated protein kinase (MAPK, extracellular signal-regulated kinase [ERK]) and phosphatidylinositide 3-kinase (PI3-K)/Akt-1 pathways (5–7). These can stimulate tumor progression and cellular differentiation (8). IGF-IR axis function is also regulated by IGF binding proteins (IGFBPs) and type 2 IGF receptor (IGF-IIR; refs. 9–11).

Authors' Affiliations: [1]First Department of Internal Medicine, Sapporo Medical University, Sapporo, Japan; Departments of [2]Medicine and [3]Cell Biology, Vanderbilt-Ingram Cancer Center and Vanderbilt University, Nashville, Tennessee; and [4]The Institute of Medical Science, The University of Tokyo, Tokyo, Japan

Note: M. Ii, H. Li, and Y. Adachi contributed equally to this work.

Corresponding Author: Yasushi Adachi, First Department of Internal Medicine, Sapporo Medical University, S-1, W-16, Chuo-ku, Sapporo 060-8543, Japan. Phone: +81-11-611-2111(ext. 3211); Fax: +81-11-611-2282; E-mail: yadachi@sapmed.ac.jp

doi: 10.1158/1078-0432.CCR-10-3131

Published OnlineFirst June 3, 2011; DOI:10.1158/1078-0432.CCR-10-3131

Translational Relevance

IGF-IR signaling is important for tumorigenicity and progression of many cancers and *k-ras* mutation is one of key factors in gastrointestinal cancers. Drugs targeting for IGF-IR pathways is in trial evaluation. In this report, we revealed that the IGF-IR monoclonal antibody, figitumumab (CP-751,871), inhibited signal transduction, proliferation, and survival of 6 gastrointestinal cancer cell lines. Moreover, in addition to its monotherapy, the combination of figitumumab and chemotherapies was highly effective against these xenograft tumors on mice. The effect of figitumumab is not influenced by the mutation status of *k-ras*. This study suggests that figitumumab may have therapeutic value in human gastrointestinal carcinomas even in the presence of *k-ras* mutations.

IGFs stimulate the proliferation of GI cancer cells and blocking of IGF-IR signaling inhibits tumor growth (9, 12–20). High serum concentration of IGF-I increases the risk of developing several cancers (10). IGF-I can also antagonize the antiproliferative effects of cyclooxygenase-2 (COX-2) inhibitors (21). Soluble IGF-IIR salvages Apc (Min/+) intestinal adenoma progression induced by loss of IGF-II imprinting (11). IGF-IR is also important for tumor maintenance in addition to carcinogenicity (22, 23). Intestinal fibroblast-derived IGF-II has been shown to stimulate proliferation of intestinal epithelial cells (24). IGF-II, in conjunction with IGF-IR, IGF-I, COX-2, and matrilysin (matrix metalloproteinase-7), seems to play a key role in the early stages of colorectal carcinogenesis (25, 26). IGF-IR signaling is also critical in tumor dissemination through the control of adhesion, migration, and metastasis. Matrilysin can cleave all 6 IGFBPs and can thus cause activate IGF signals (27, 28). We have previously reported a positive feedback loop between the IGF/IGF-IR axis and matrilysin in the invasiveness and progression of GI cancers (29).

The insulin receptor (InsR) is also another key molecule of the IGF signaling pathway and leads cell proliferation as well as affecting glucose metabolism. In addition to insulin, InsR can also bind IGF-II and initiate mitogenic signals (30). IGF-IR and InsR can form hybrid receptors that bind IGFs at physiologic concentrations. InsR and these hybrid receptors may also be involved in tumor as both insulin and IGF-I contribute to the development and progression of adenomas (31).

There are several possible approaches to blocking the IGF-IR axis. Humanized or human mAbs and TKIs for IGF-IR are available and some are in phase trials (32–34). We have constructed 2 dominant negative inhibitors for IGF-IR (IGF-IR/dn), which are active as plasmids and recombinant adenovirus vectors for several GI malignancies (15, 35–37). Figitumumab (CP-751,871) is a highly specific, fully human mAb that inhibits ligand-induced IGF-1R autophosphorylation (32). Phase 1 trials reveal that this mAb has a favorable pharmacodynamic profile and is well tolerated as a single drug without dose-limiting toxicities (38, 39). Figitumumab is also tolerable in combination with paclitaxel, carboplatin, or docetaxel (40, 41). There are only 3 reports about the efficacy of figitumumab on human GI malignancies, 1 colorectal cancer cell line, colo205, and 2 clinical studies for patients with solid tumors, including esophageal, gastric, and colon cancers and GI stromal tumor (32, 38, 42). As GI cancers are heterogeneous diseases, we decided to analyze the utility of this compound in several human GI cancer cell lines.

On the other hand, cetuximab, which is a mAb for epidermal growth factor receptor, is a useful drug for patients with colorectal cancer, however, it is not effective for tumors bearing *k-ras* mutations (43, 44). Mutation in *k-ras* is a critical genetic change, as the incidence of *k-ras* mutation is 40% to 45% in colon cancer and around 90% in pancreatic cancer. However, there is no report regarding the efficacy of IGF-IR targeting therapies for *k-ras* mutated cancers.

In this study, we assessed the impact of figitumumab on signaling blockade, growth, apoptosis-induction, and *in vivo* therapeutic efficacy in s.c. xenografts for GI cancers. We also analyzed the effects of this drug in cell lines with *k-ras* mutations. These observations strengthen the rationale for using figitumumab alone or in combination with chemotherapy in the molecular targeted therapy of GI cancers.

Materials and Methods

Materials, cell lines, and mice

Anti-Akt1(c-20), anti-ERK1(K-23), anti-phospho-ERK1 (E-4), ant-IGF-I(G-17), anti-IGF-IRα(2C8), and anti-IGF-IRβ(C20) were purchased from Santa Cruz Biotechnology and anti-phospho-Akt(Ser473), anti-phospho-p44/42-MAPK(Thy202/Tyr204), and PathScan Multiplex Western Cocktail-I were from Cell-Signaling Technology. 5-Fluorouracil (5-FU) was purchased from Sigma. Recombinant human IGF-I and IGF-II was purchased from R&D systems. All human GI cancer cell lines, colon adenocarcinomas, HT29 and DLD-1; pancreatic adenocarcinomas, BxPC3 and MIAPaca2; esophageal squamous cell carcinoma (ESCC), TE-1; and hepatoceller carcinoma, PLC/PRF/5 were obtained from Japanese Cancer Collection of Research Bioresources Cell Bank. Cells were passaged in RPMI1640 and DMEM with 10% FBS. Specific-pathogen-free female BALB/cAnNCrj-nu mice, 6-weeks-old, were purchased from Charles River. The care and use of mice were according to our university's guidelines.

A new monoclonal antibody for IGF-IR, figitumumab (CP-751,871), was kindly provided by Pfizer.

Western blotting

To analyze the duration of efficacy of this antibody, cells were cultured with media containing 0.1% bovine serum albumin and were incubated several hours with 1 μg/mL figitumumab before ligand stimulation. To assess the concentration of figitumumab required to block

Published OnlineFirst June 3, 2011; DOI:10.1158/1078-0432.CCR-10-3131

ligand-induced signal transduction, cells were cultured with media containing 0.1% bovine serum albumin and were incubated 0.5 to 3 hours with several concentrations of this mAb before stimulation.

Cells were treated with 20 ng/mL IGF-I, 40 ng/mL IGF-II, or 10 nmol/L insulin 5 minutes. Cell lysates were prepared as described previously (35). Equal aliquots of lysates (100 μg) were separated by 4% to 20% SDS-PAGE and immunoblotted onto polyvinylidene Hybond-P membrane (Amersham). Analysis was performed using indicated antibodies, and bands visualized by ECL (Amersham).

Colony-forming activity

Cells (3×10^3/plate) were seeded onto 60 mm culture plates and incubated for 24 hours. The cells were then treated with figitumumab and were incubated for 14 days. After air drying, cells were fixed with methanol and stained with Giemsa solution. Colonies containing 50 cells or more were counted.

Assessment for apoptosis

The caspase-3 colorimetric protease assay was performed following the manufacturer's protocol (MBL). In brief, the caspase-3 activity of lysates (100 μg) was measured by colorimetric reaction at 400 nm. Early apoptosis were quantified by staining with Anexin-V-FITC, according to the manufacturer's protocol (BD Biosciences) and measured by flow cytometry. TUNEL assays were performed with *in situ* apoptosis detection kit (Takara), following the manufacturer's protocol.

In vivo therapeutic efficacy in established tumors

A total of 1×10^6 GI cancer cells were s.c. injected into nude mice. After tumors were palpable, animals were treated with intraperitoneal (i.p.) injection of 125 μg figitumumab, twice a week or control. Tumor diameters were serially measured with calipers and tumor volume was calculated using the formula: tumor volume (mm^3) = (width^2 × length)/2.

After GI tumors were palpable, animals were treated with i.p. injection of 125 μg figitumumab, twice a week or control. Both groups were then divided into pair-matched cytotoxic drugs, 50 mg/kg 5-FU (administered i.p. once per week) or 100 mg/kg gemcitabine (i.p., twice a week), treated and control groups. Mice were euthanized when tumors reached 2 cm in size or they developed clinically evident symptoms.

Immunohistochemical analysis

Sections (5 μm) from formalin-fixed, paraffin-embedded tumor xenografts were prepared. After removed paraffin, the sections were pretreated with Dako-Cytomation Target Retrieval Solution (Dako) in a microwave (10 minutes). Then, endogenous peroxidase activity was blocked. Antibodies were applied after blocking with normal goat serum. Sections were incubated with the anti-rabbit secondary antibody (Santa Cruz Biotechnology) and a streptavidin-HRP (Dako) followed by exposure to the diaminobenzidine tetrahydrochloride substrate (Dako).

ELISA

Serum concentrations of IGF-I, GH, insulin, and IGFBP-3 were measured using the following ELISA kits, following the manufacturer's protocols; mouse IGF-I Quantikine (R&D Systems), mouse growth hormone kit (Uscn Life Science & Technology), mouse insulin kit (Shibayagi), and mouse- and rat-IGFBP-3 ELISA (Mediagnost).

Statistical analysis

The results are presented as mean ± SE for each sample. The statistical significance of differences was determined by Student's 2-tailed *t* test in 2 groups and done by 1-way ANOVA in multiple groups, and 2-factor factorial ANOVA. *P* values of less than 0.05 were considered to indicate statistical significance.

Results

Blockade of signal transduction

To investigate the effect of figitumumab on the IGF/receptor axis, we examined 2 GI cancer cell lines, a pancreatic cancer cell, BxPC3 and a colorectal cancer cell line, HT29, which we used to evaluate the efficacy of IGF-IR blockade in the previous studies (36, 37). First, we assessed effects of figitumumab in BxPC3 on activation of IGF-IR and its downstream signals by immunoblotting. Low concentration of 0.1 μg/mL figitumumab blocked IGF-I–induced phosphorylation of both IGF-IR and Akt-1 and reduced phosphorylation of ERKs (Fig. 1A).

Similarly, in HT29 cells, figitumumab eliminated ligand-induced IGF-IR autophosphorylation and phosphorylation of both downstream, Akt-1 and ERKs (Fig. 1B). The results indicate that this mAb might effectively inhibit the IGF axis in both BxPC3 and HT29.

Then, the effect of figitumumab on a hepaloma cell line, PLC/PRF/5, was assessed (Fig. 1C). This mAb blocked both IGF-IR downstream signals of Akt-1 and ERKs with a dose dependency. One μg/mL figitumumab blocked autophosphorylation of IGF-IR and the downstream signals from 1 to 48 hours.

The *in vitro* effect on cell growth and survival

Then we analyzed the effect of this drug on *in vitro* growth and survival. One μg/mL figitumumab dramatically reduced the *in vitro* tumorigenicity of 3 cell lines as assessed by the colony formation assay (Fig. 2A).

Annexin-V assays revealed that this mAb up-regulated ethanol-induced early apoptosis synergistically in HT29 (Fig. 2B). Then we evaluated the effect of this drug on chemotherapy-induced apoptosis. Caspase-3 assay revealed that figitumumab enhanced 5-FU induced apoptosis synergistically in both HT29 and BxPC3 (Fig. 2C). The antibody strengthened additively the effect of gemcitabine

Published OnlineFirst June 3, 2011; DOI:10.1158/1078-0432.CCR-10-3131

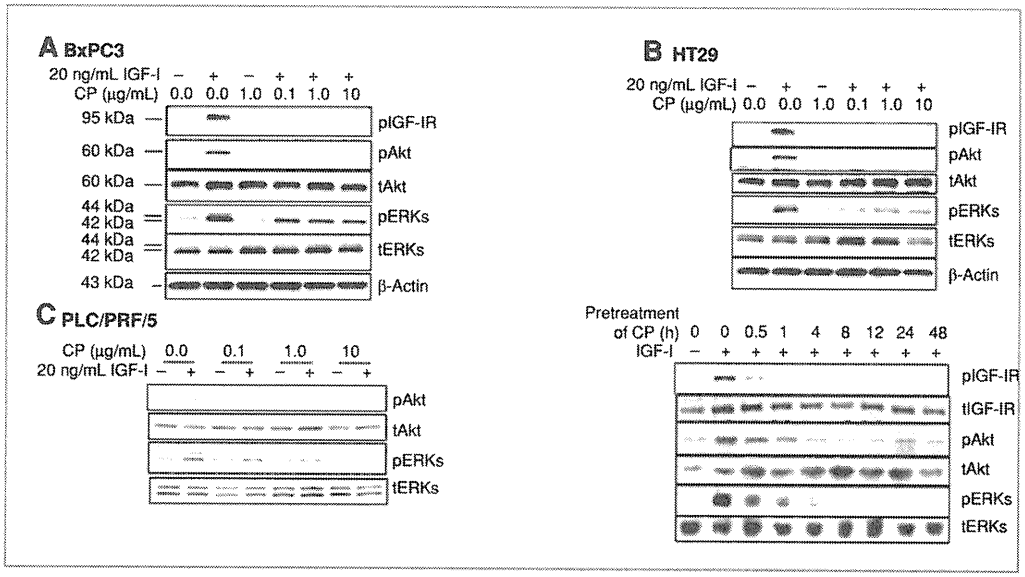

Figure 1. Two gastrointestinal cancer cell lines, pancreatic adenocarcinoma, BxPC3 (A), and colorectal adenocarcinoma, HT29 (B) were cultured with different doses of figitumumab 30 minutes, then were stimulated with 20 mg/mL IGF-I 5 minutes. Western blotting shows that CP-751,871 blocks IGF-I–induced autophosphorylation of IGF-IR completely in both cells. Figitumumab terminated IGF-I–induced activation of and Akt-1, but not ERKs completely. C, in hepatocellular carcinoma, PLC/PRF/5, ligand induced both phospholyration of Akt and ERKs were blocked by 3 hours treatment with this mAb. With incubation with 1 μg/mL figitumumab from 1 to 48 hours, this agent effectively blocked IGF-I–stimulated autophosphorylation of IGF-IR and both activation of Akt and ERKs in PLC/PRF/5.

in BxPC3 and that of 5-FU in PLC/PRF/5 (Fig. 2C). These data suggest that figitumumab might have several *in vitro* antitumor effects on GI cancer cells.

Figitumumab suppresses xenograft tumors

To analyze the effect of this drug on *in vivo* GI cancer, HT29 cells were inoculated s.c. in nude mice and allowed to

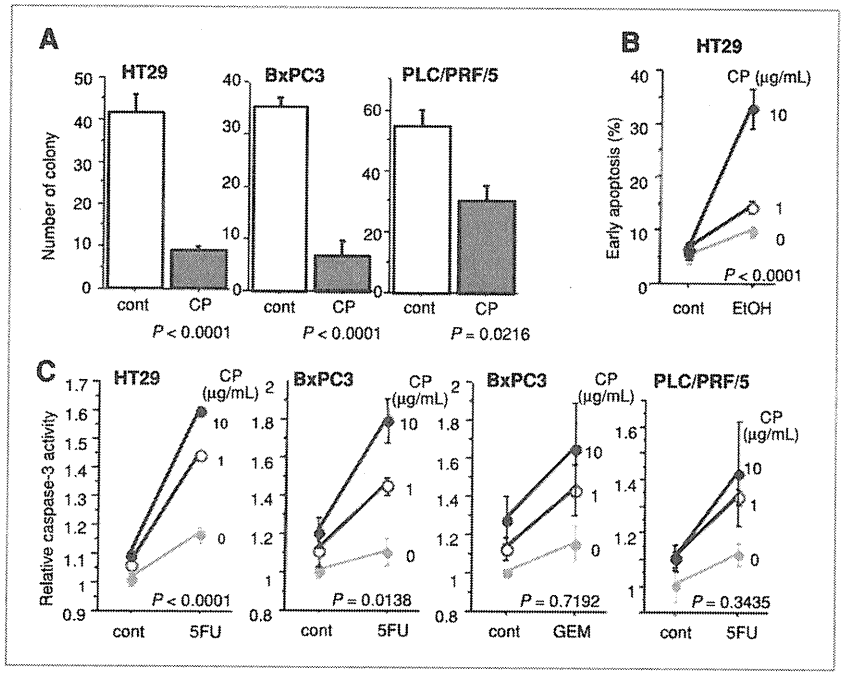

Figure 2. The effects of figitumumab on colony formation and apoptotic induction. A, colony formation assay shows that 1 μg/mL CP-751,871 reduced the number of colony of 3 GI cancer cell lines. B, Anexin-V assay reveled that CP-751,871 strengthen ethanol induced apoptosis synergistically in HT29. C, caspase-3 assay shows that CP-781871 enhanced 5-FU induced apoptosis synergistically in HT29 and BxPC3, and did additively in PLC/PRF5. Cont, control; CP, CP-751,871 (figitumumab); Gem, gemcitabine.